BMC Plant Biology

RESEARCH

Open Access

# Genome-wide identification of kiwifruit $K^+$ channel *Shaker* family members and their response to low-$K^+$ stress

Yinqiang Zi[1†], Zhiming Zhang[2†], Ke Zhao[1], Xiuyao Yang[1], Ling Zhu[1], Tuo Yin[1], Chaoying Chen[1], Ke Wen[1], Xulin Li[1], Hanyao Zhang[1*] and Xiaozhen Liu[2*]

## Abstract

**Background** 'Hongyang' kiwifruit (*Actinidia chinensis* cv 'Hongyang') is a high-quality variety of *A. chinensis* with the advantages of high yield, early ripening, and high stress tolerance. Studies have confirmed that the *Shaker* $K^+$ genes family is involved in plant uptake and distribution of potassium ($K^+$).

**Results** Twenty-eight *Shaker* genes were identified and analyzed from the 'Hongyang' kiwifruit (*A. chinensis* cv 'Hongyang') genome. Subcellular localization results showed that more than one-third of the *AcShaker* genes were on the cell membrane. Phylogenetic analysis indicated that the *AcShaker* genes were divided into six subfamilies (I-VI). Conservative model, gene structure, and structural domain analyses showed that *AcShaker* genes of the same subfamily have similar sequence features and structure. The promoter cis-elements of the *AcShaker* genes were classified into hormone-associated cis-elements and environmentally stress-associated cis-elements. The results of chromosomal localization and duplicated gene analysis demonstrated that *AcShaker* genes were distributed on 18 chromosomes, and segmental duplication was the prime mode of gene duplication in the *AcShaker* family. GO enrichment analysis manifested that the ion-conducting pathway of the *AcShaker* family plays a crucial role in regulating plant growth and development and adversity stress. Compared with the transcriptome data of the control group, all *AcShaker* genes were expressed under low-$K^+$stress, and the expression differences of three genes (*AcShaker15*, *AcShaker17*, and *AcShaker22*) were highly significant. The qRT-PCR results showed a high correlation with the transcriptome data, which indicated that these three differentially expressed genes could regulate low-$K^+$ stress and reduce $K^+$ damage in kiwifruit plants, thus improving the resistance to low-$K^+$ stress. Comparison between the salt stress and control transcriptomic data revealed that the expression of *AcShaker11* and *AcShaker18* genes was significantly different and lower under salt stress, indicating that both genes could be involved in salt stress resistance in kiwifruit.

[†]Yinqiang Zi and Zhiming Zhang contributed equally to this work

*Correspondence:
Hanyao Zhang
zhanghanyao@swfu.edu.cn
Xiaozhen Liu
15198729095@swfu.edu.cn

Full list of author information is available at the end of the article

**Conclusion** The results showed that 28 *AcShaker* genes were identified and all expressed under low $K^+$ stress, among which *AcShaker22* was differentially and significantly upregulated. The *AcShaker22* gene can be used as a candidate gene to cultivate new varieties of kiwifruit resistant to low $K^+$ and provide a reference for exploring more properties and functions of the *AcShaker* genes.

**Keywords** 'Hongyang' kiwifruit, *Shaker* genes, Transcriptome, low-$K^+$ stress, Salt stress, Expression pattern

## Introduction

Kiwifruit is a plant of the genus Actinidia in the family Actinidiaceae [1, 2]. It has a high vitamin content and is known as the 'king of fruits' [3, 4]. Kiwifruit is one of several fruits that has been successfully adopted by the international market in recent years; it is the most widely grown and economically valuable cultivar in the world, and it is a high-value export crop for countries such as New Zealand, Italy, and Chile [5]. China is the prime source of wild kiwifruit and the largest producer of kiwifruit [6]. 'Hongyang' kiwifruit (*A. chinensis* cv 'Hongyang') is the first new red-fleshed kiwifruit variety selected and bred by the Cangxi County Agricultural Bureau of Guangyuan City, Sichuan Province, and the Sichuan Institute of Natural Resources, and it is a high-quality variety of *A. chinensis* [7]. With early ripening, high yield, and suitability for a wide range of plantings, 'Hongyang' kiwifruit is rich in nutrients and has high economic value and development prospects.

Potassium (K) is an essential macroelement for plant growth and is second only to nitrogen (N) in its internal content [8]. $K^+$ has a direct regulatory effect on stomatal opening and closing and cellular water uptake [9]. In 1943, Boyer et al. [10] first reported the ability of $K^+$ to catalyze the activation of pyruvate kinase. More than 60 enzymes, including synthases, transferases, and oxidases, are known to require $K^+$ as an activator and thus participate in the synthesis and metabolism of plant proteins. Previous studies showed that $K^+$ is also involved in the H+-ATPase enzyme activation, which allows $K^+$ to pass through the plasma membrane from the extracellular solution into the cell, suggesting that $K^+$ can facilitate the transmembrane transport of intracellular substances [11]. Kaiser et al. [12] and Pier and Berkowitz [13] reported that the color effect of $K^+$ on photosynthesis is also manifested in the rate at which $CO_2$ is fixed by photosynthesis; when the external $K^+$ concentration increases, the rate at which $CO_2$ is fixed by photosynthesis increases; conversely, the opposite is true. Fontana et al. [14] reported that K deficiency significantly affects the growth and development of cotton plants, as evidenced by a reduction in plant height and total leaf-root area and further reduced fresh and dry biomass of the whole plant. The results of tomato soilless culture experiments suggested that K can reduce the negative effects of Cd by improving photosynthesis and promoting chlorophyll synthesis, and optimizing nutrient composition and concentration may be a better strategy for reducing the impact of Cd on plant growth and physiology [15]. In addition, $K^+$ plays the most vital role in improving plant protein stability [16]. As an opposite-phase charged ion, $K^+$ is usually involved in the long-range transport of $NO_3^-$ in the xylem and the storage of $NO_3^-$ in vesicles; in plants, after the reduction of $NO_3^-$, comparable organic acids are synthesized from $K^+$ to maintain intracellular charge balance and pH stability [17, 18]. $K^+$ can promote the release of photosynthates from chloroplasts or directly affect the activity of ATPase in sieve tubes, and it can also regulate the osmotic potential of photosynthates from source to reservoir by increasing the pH in the sieve tubes of the phloem [19].

Despite the abundance of $K^+$ in the soil, $K^+$ uptake and utilization by plant roots are low, resulting in lower crop yields [20, 21]. Potash resources are scarce in China, and most potassium is imported. The shortage of potassium in the soil has become a prime factor limiting agricultural development in China and the world [22].

In $K^+$-deficient plants, sucrose loading in the phloem is inhibited [23, 24], and sucrose transport to the roots is reduced, resulting in a significant decrease in the root sucrose concentration [25]. Under $K^+$ deficiency stress, the rate of outward transport of photosynthesis products is significantly reduced, forcing a significant increase in the content of photosynthesis products in the source leaves [25, 26]. Therefore, the growth and development of aboveground plant parts and the root system are inhibited [27]. Severely $K^+$-deficient plants wilt, and the cell wall lignification process is blocked. As a result, the cells are more susceptible to fungal infestation, ultimately leading to lower yield and quality [21].

*Shaker* channels are considered the most vital proteins for maintaining $K^+$ in plants, and they are involved in $K^+$ nutrient uptake, regulation of intracellular $K^+$ homeostasis, and transport [28]. The first $K^+$ channel gene, *AKT*, was cloned in *A. thaliana* [29] and plays a vital role in $K^+$ uptake and tolerance to low-$K^+$ stress and adapts to high salt environments by maintaining intracellular $K^+$/$Na^+$. Similarly, Ródenas et al. [30] noted that the *AtSKOR* potassium channel mediates potassium transport to the xylem and is significantly upregulated under salt stress, thereby increasing salt tolerance. Nine *shaker* gene family members have been identified in *A. thaliana* and are categorized into five subfamilies based on their role in $K^+$ channel proteins [31]. Currently, with the development of

genomics and genetics, the study of the *shaker* $K^+$ channel protein-encoding gene family has been completed with genome-wide identification and analysis in a variety of plants, including cabbage [32], cereal [33], Rosa canina [34], and sweet potato [35]. The *shaker* gene family plays a vital role in $K^+$ uptake and stress resistance [32]. Chen et al. showed that the *GmAKT1* gene increased the tolerance of soybeans to abiotic stresses [36]. Domestic researchers have found that the *IbAKT* gene may play a crucial role in $K^+$ deficiency tolerance regulation in sweet potatoes [35]. More *Shaker* family genes have been identified in plants, the understanding of *Shaker* family genes has gradually deepened, and the biological functions of these genes have been elucidated. However, there are no relevant studies on the *Shaker* gene family in kiwifruit.

This study aimed to comprehensively analyze the identification, physicochemical property analysis, phylogenetic analysis, gene structure, structural domains and conserved motifs, cis-acting regulatory elements, chromosomal localization, gene duplication, covariate analysis, and GO enrichment analysis of *Shaker* family members across the whole genome of kiwifruit and to explore the expression pattern of kiwifruit in response to low-$K^+$ and salt stress. This study lays the foundation for understanding the evolution and biological functions of the *Shaker* transcription factor family in kiwifruit. Moreover, this study provides a primary basis for further research on breeding for kiwifruit resistance to low-$K^+$ stress.

## Materials and methods

### Plant materials

'Hongyang' kiwifruit from the Aziying orchard, Panlong District, Yunnan Province, were selected as explants, and kiwifruit seedlings were obtained by histoculture techniques. *A. chinensis* 'Hongyang' was cultivated from seedlings collected from an orchard in Henan Province by the Institute of Natural Resources of Sichuan Province and Guangxi County Agricultural Bureau of Sichuan Province. It has excellent traits, such as a large fruit, thin skin, fast growth, early maturity, and red flesh [7].

### Access to data

The 'Hongyang' kiwifruit genetic data were downloaded from the kiwifruit gene database KGD: Kiwifruit Genome Database (http://kiwifruitgenome.org/) (*Actinidia chinensis* (Hong Yang V3)). Sequence information on the conserved structural domains of the *Shaker* gene family (ID: PF00027, ID: PF00520, ID: PF11834) was downloaded from the Pfam website (http://pfam.xfam.org/), and hidden Markov model files were constructed using the HMMER3 soft package [33]. The protein sequences and genomic data of nine *Arabidopsis Shaker* $K^+$ channel protein families were downloaded from the *Arabidopsis* genome website TAIR (https://www.Arabidopsis.org/) [34].

### Identification and physicochemical characterization of kiwifruit *shaker* gene family members

Based on the data downloaded from the above steps, the BLAST program in TBtools software was used to perform a BLAST comparison of the kiwifruit genomic protein data using the protein sequences of the *Arabidopsis Shaker* gene family as a reference. The protein sequences in the kiwifruit genomic protein data that had high homology (E-value$<1\times10^{-5}$) sequences were screened out [37]. Second, the hmmsearch program was used to search the kiwifruit genome-wide protein structural domains (ID: PF00027, ID: PF00520, ID: PF11834), and protein sequences with an E-value of $<1\times10^{-5}$ were filtered out [38]. Finally, the protein sequence number columns obtained in the above two steps were combined, and duplicates were selected. The selected protein sequences were extracted from the kiwifruit gene protein database using the TBtools tool to obtain the corresponding sequences, which were saved as *.fast files [37]. The online protein structural domain analysis tools SMART (http://smart.embl-heidelberg.de/) and CDD (https://www.ncbi.nlm.nih.gov/Structure/cdd/wrpsb.cgi) were used to determine whether the candidate sequences contained *Shaker* structural domains [39], and the missing or incomplete structural domains were eliminated to obtain the kiwifruit *Shaker* gene family members. The identified *Shaker* genes were renamed according to their chromosomal locations and named *AcShaker*+sequence number. The obtained protein sequences were submitted to the ExPASy ProtParam (https://web.ExPASy.org/protparam/) online tool for the detection of physicochemical properties such as protein sequence length, relative molecular weight, theoretical isoelectric point, and hydrophilicity. Finally, subcellular localization analysis was performed using WoLF PSORT (https://wolfpsort.hgc.jp/) [40]. TBtools was utilized to calculate the gene length and coding region length 2000 bp upstream of the encoded gene [37].

### Phylogenetic analysis of the kiwifruit *Shaker* gene family

To understand the evolutionary relationship between kiwifruit and *Arabidopsis Shaker* gene families. The sequences of the *Shaker* $K^+$ proteins obtained from kiwifruit and *A. thaliana* were combined, and an amino acid sequence phylogenetic tree of 28 kiwifruit *Shaker* proteins (*AcShaker*) and nine *A. thaliana Shaker* proteins [38] was constructed using the neighbor-joining (NJ) method with a bootstrap value of 1000. The bootstrap value was 1000. The phylogenetic tree was built using the iTOL (https://itol.embl.de/) online tool [41]. Finally, 28 *Shaker* proteins of kiwifruit were grouped according

to the grouping of *Arabidopsis Shaker* $K^+$ channel proteins [42]. The amino acid sequences of *AcShaker22* and *AtAKT1* were subjected to multiple sequence comparisons using MAFFT (version 7.5) comparison software, and the results were visualized using Geneious (version 9.1.4) comparison [43, 44]. The tertiary structures of the *AcShaker22* and *AtAKT1* proteins were constructed using SWISS-MODEL (https://swissmodel.ExPASy.org/).

#### Analysis of gene structure, structural domains, and conserved motifs

Based on the genome annotation file (GFF3) of kiwifruit, TBtools software was used to analyze the gene structure of each gene [36]. The structural domains of the kiwifruit *Shaker* $K^+$ channel proteins were then predicted using the CD-search online tool (http://www.ncbi.nlm.nih.gov/Structure/bwrpsb/bwrpsb.cgi) from the NCBI database with default parameters [45]. Motif analysis of *AcShaker*-encoded proteins was performed using the online tool MEME (https://meme-suite.org/meme/) [46] (the maximum number of conserved motifs retrieved was ten, and the other parameters were the defaults) to analyze the differences between members of the *Shaker* gene family. Finally, the above results were visualized by TBtools software.

#### Analysis of cis-acting elements

To analyze the cis-acting elements in the promoter region of the *AcShaker* genes, the base sequences 2000 bp upstream of each gene were extracted separately from the genome annotation file (GFF3) using TBtools software, and then the promoter cis-acting element analyses were carried out using the online analysis software PlantCARE (https://bioinformatics.psb.ugent.be/webtools/plantcare/HTML/) [47].

#### Chromosome localization and covariance analysis

Chromosome position information was obtained from the genome annotation file (GFF3), and chromosome position mapping was performed by TBtools software. The chromosome length information, position information, and density information of the *AcShaker* gene were extracted by TBtools, and the intraspecific covariance of *AcShaker* family members was analyzed using MCSanX in TBtools software [37].

#### GO functional enrichment analysis of the *Shaker* genes

Based on the kiwifruit whole-genome protein sequence files, the protein sequences of the *AcShaker* protein-encoding gene family were extracted, and the proteins of the 28 *AcShaker* genes were functionally annotated through the EggNOG-MAPPER database (http://eggnog-mapper.embl.de/) [48]. The *Shaker* gene families of kiwifruit were then subjected to GO functional enrichment analysis using TBtools and plotted and visualized by the online tool ChiPlot (https://www.chiplot.online/bar_plot_width_category) [49].

#### Expression pattern analysis of Kiwifruit *Shaker* genes in response to low-$K^+$ and salt stress

##### *Determination of low-$K^+$ and salt concentrations*

In the MS media, the $K^+$ in the media was reduced by decreasing the concentration of $KNO_3$ and increasing the appropriate concentration of $NH_4NO_3$ to compensate for the loss of $NO_3^-$ from $KNO_3$. With the modified 'Hongyang' kiwifruit MS medium by Wu et al., 'Hongyang' kiwifruit histocultured seedlings grew best in the $NH_4NO_3$ concentration range of 250 mg/L −650 mg/L, and the MS medium with $NH_4NO_3$ concentration in MS medium was 450 mg/L [50]. A concentration of $KNO_3$ in the 300 mg/L-700 mg/L was the best for growth [51]. In this experiment, a one-way experimental design was adopted, and the concentrations of $KNO_3$ were 300 mg/L, 250 mg/L, 200 mg/L, 150 mg/L, and 100 mg/L, with corresponding $NH_4NO_3$ concentrations of 450 mg/L, 500 mg/L, 550 mg/L, 600 mg/L and 650 mg/L, respectively. Regular MS medium was used as the control to screen out the best $K^+$-deficient formula. The optimum $K^+$-deficient formulation was screened. Tissue culture-generated seedlings with roughly equal root lengths were selected and cultured in media supplemented with different concentrations of $K^+$. Each bottle was inoculated with one plant, and three replicates were made for each combination. Each replicate had ten bottles of seedlings, which were randomly placed in the incubation room at 26±1 °C after inoculation. After inoculation, the plants were randomly placed in an incubation room at 26±1 °C. Phenotypic changes were observed, and growth was measured every 5 d.

##### *Phenotypic observations of $K^+$-deficient kiwifruit leaves and roots*

Sixty ordinary plants with almost uniform growth were randomly selected, and 30 were placed in $K^+$-deficient or regular media. The number of roots per plant was controlled to three, and the excess root hairs were removed before the plants were planted in the media. The plant roots were placed close to the surface of the culture medium. After 30 d of incubation, the seedlings were removed. Then, the number of roots, number of root hairs, and number of red leaves were observed and statistically analyzed.

##### *Low-$K^+$ and salt stress treatments and transcriptome sequencing*

A total of 18 ordinary plants with almost uniform growth were randomly selected, and nine were added to $K^+$-deficient or regular media. After 10 d of incubation

[49], the seedlings were removed. Then, the roots of the plants were removed in liquid nitrogen for transcriptome sequencing. Nine plants in $K^+$-deficient culture media were randomly grouped into T1, T2, and T3, and nine plants in regular culture media were randomly grouped into CK1, CK2, and CK3. Each group contained three sample plants, and the roots of each sample plant were taken as the experimental materials in turn. The samples were removed, stored on dry ice, and then sent to BQ Biotech for transcriptome sequencing and analysis.

Twelve kiwifruit histocultures with 4–5 leaves were selected and treated with salt (NaCl). Before the experiments, many pretests were carried out to determine the optimal NaCl concentration (3 g/L). The salt treatment times were set at 24 h, 48 h, and 72 h for the T1, T2, and T3 groups, respectively, and a salt treatment time of 0 h was used for the CK group. Three biological replicates were performed for each group. The samples were sequentially removed and stored in liquid nitrogen for transcriptome sequencing and analysis by Wuhan Baiyihui Energy Biotechnology Co., Ltd. TBtools software (version 2.012) was used to construct heatmaps.

#### Expression pattern analysis of the *Shaker* gene family in 'Hongyang' kiwifruit plants under low-$K^+$ and salt stresses

The whole genome of *A. chinensis* was selected as the reference genome for transcriptome sequencing data, and Bowtie2 software was used for sequence comparison. The comparison results of Bowtie2 were statistically analyzed to obtain the number of reads compared to each transcript for each sample using RSEM v1.3.0 software [52], and the average expression level (fragments per kilobase per million bases, FPKM) conversion was calculated for each transcribed region. Paired-end reads from the same fragment were counted as fragments, which provided the expression level EXPECTED count data for genes and transcripts, where genes with FPKM values greater than 0 were considered expressed genes. The domain p value was determined by controlling the FDR (false discovery rate) [53]. Then, using the read count information, differentially expressed genes (DEGs) were analyzed using the R package edge R. The genes with thresholds of FDR < 0.05, $\log_2$FC > 1, or $\log_2$FC < -1 were screened as the final DEGs.

#### qRT-PCR analysis

To further validate the accuracy of the transcriptome data, we selected ten genes (including *AcShaker15*, *17*, and *22*) whose expression significantly differed under low-$K^+$ stress for qRT-PCR validation. Kiwifruit leaves cultured in regular media for 10 d composed the control group (CK1, CK2, and CK3), and kiwifruit leaves cultured in low-$K^+$ media for 10 d composed the treatment group (T1, T2, and T3). Total RNA was extracted using a Vazyme kit (Nanjing, China) from Novozymes Biotechnology Co., Ltd. To reverse-transcribe total RNA into cDNA for qRT-PCR analysis, HiScript®ll QRT SuperMix was used for qPCR (+gDNA wiper) (R223-01) for the First Strand Synthesis Kit. The qRT-PCR primers (Table S1) were then designed using Primer 6.0. The WDR1 gene was used as an internal reference gene for standard RT-qPCR using the ChamQ Universal SYBR qPCR Master Mix (Q711-02) kit with three replicates per gene. Finally, expression analysis was performed using the $2^{-\Delta\Delta Ct}$ method.

## Results

#### Identification and physicochemical characterization of kiwifruit *Shaker* gene family members

BLAST and hmmsearch searches were performed on kiwifruit genomic protein data using protein sequences of the *Arabidopsis Shaker* $K^+$ channel protein-encoding gene family as a control. Next, the kiwifruit *Shaker* gene family was predicted by CDD and Pfam to remove missing or absent structural domains, and a total of 28 *Shaker* genes were ultimately identified. These genes were named *AcShaker1-AcShaker28* according to their chromosomal positions. Further analysis of the AcShaker protein sequences revealed that the protein lengths of the *Shaker* genes varied considerably, ranging from 338 (*AcShaker12*)-900 (*AcShaker30*) amino acids; the molecular weights ranged from 14.21 (*AcShaker23*)-100.69 (*AcShaker30*) kDa; the pI ranged from 4.36 (*AcShaker23*)-9.87 (*AcShaker6*); and the instability coefficients ranged from 25.66 (*AcShaker23*)-56.83 (*AcShaker11*). A total of nine genes, *AcShaker5*, *AcShaker11*, *AcShaker15*, *AcShaker17*, *AcShaker18*, *AcShaker20*, *AcShaker22*, *AcShaker27*, and *AcShaker28*, had instability coefficients less than 40, which indicated that they were stable proteins, and the other *AcShaker* genes were all unstable proteins. Second, $K^+$ can improve the stability of proteins [16]; the lipolysis index ranged from 77.82 (*AcShaker6*) to 101.15 (*AcShaker4*) (Table 1). The subcellular localization prediction of the Plant-mPLoc tool showed that nine *AcShakers* were located in the cell membrane. Plant $K^+$ uptake requires the involvement of a membrane [20], which is favorable for improving the efficiency of $K^+$ uptake in plants. Twelve *AcShakers* were located in the nucleus, four *AcShakers* were located on chloroplasts, and the remaining three *AcShakers* were located on the plasma membrane, Golgi apparatus, and extracellular matrix (Fig. 1, Table S2).

#### Phylogeny of the kiwifruit *Shaker* gene family

To understand the evolutionary relationship between the kiwifruit *Shaker* gene family and other *Shaker* gene families, 28 kiwifruit Shaker protein sequences were aligned with 9 *Arabidopsis* Shaker protein sequences.

**Table 1** Analysis of physicochemical properties of AcShaker TFs

| Sequence ID | Gene name | Number of amino acids(aa) | Molecular weight(kDa) | Theoretical pI | Instability index | Aliphatic index | Subcellular Localization |
|---|---|---|---|---|---|---|---|
| Actinidia24029 | *AcShaker1* | 403 | 46.61 | 9.01 | 49.83 | 87.59 | Cell membrane |
| Actinidia09058 | *AcShaker2* | 756 | 86.47 | 6.18 | 40.86 | 92.24 | Nucleus |
| Actinidia19524 | *AcShaker3* | 771 | 87.79 | 6.91 | 42.4 | 90.4 | Nucleus |
| Actinidia39029 | *AcShaker4* | 156 | 17.70 | 5.26 | 47.66 | 101.15 | Chloroplast |
| Actinidia39030 | *AcShaker5* | 338 | 38.38 | 5.63 | 37.65 | 94.62 | Nucleus |
| Actinidia26243 | *AcShaker6* | 635 | 73.15 | 9.64 | 53.33 | 94.93 | Cell membrane |
| Actinidia03162 | *AcShaker7* | 552 | 64.01 | 9.49 | 46.56 | 92.34 | Cell membrane |
| Actinidia39406 | *AcShaker8* | 427 | 49.82 | 9.19 | 49.85 | 92.18 | Chloroplast |
| Actinidia39408 | *AcShaker9* | 663 | 76.70 | 8.93 | 47.84 | 94.09 | Cell membrane |
| Actinidia20229 | *AcShaker10* | 448 | 52.14 | 8.56 | 56.83 | 82.54 | Extracell |
| Actinidia40442 | *AcShaker11* | 876 | 98.39 | 7.05 | 36.51 | 91.19 | Nucleus |
| Actinidia17193 | *AcShaker12* | 465 | 52.80 | 6.17 | 41.72 | 94.11 | Nucleus |
| Actinidia01966 | *AcShaker13* | 701 | 80.43 | 9.58 | 50.53 | 96.09 | Cell membrane |
| Actinidia01973 | *AcShaker14* | 691 | 79.42 | 9.55 | 48.05 | 96.21 | Cell membrane |
| Actinidia00202 | *AcShaker15* | 756 | 86.27 | 7.56 | 33.24 | 98.66 | Nucleus |
| Actinidia16715 | *AcShaker16* | 786 | 89.59 | 6.75 | 41.06 | 87.34 | Nucleus |
| Actinidia14625 | *AcShaker17* | 877 | 98.33 | 7.33 | 39.65 | 94.93 | Nucleus |
| Actinidia22017 | *AcShaker18* | 585 | 64.96 | 8.13 | 39.64 | 84.39 | Chloroplast |
| Actinidia06480 | *AcShaker19* | 845 | 97.53 | 9.06 | 45.55 | 93.89 | Cell membrane |
| Actinidia32002 | *AcShaker20* | 133 | 14.21 | 4.36 | 25.66 | 77.82 | Nucleus |
| Actinidia13261 | *AcShaker21* | 876 | 99.23 | 6.42 | 44.38 | 99.2 | Nucleus |
| Actinidia13298 | *AcShaker22* | 460 | 52.50 | 5.72 | 32.36 | 96.85 | Chloroplast |
| Actinidia05145 | *AcShaker23* | 629 | 72.77 | 8.9 | 45.61 | 94.67 | Plasma membrane |
| Actinidia17572 | *AcShaker24* | 610 | 70.39 | 9.87 | 55.4 | 93.59 | Cell membrane |
| Actinidia22268 | *AcShaker25* | 736 | 84.53 | 8.24 | 49.94 | 91.3 | Cell membrane |
| Actinidia35720 | *AcShaker26* | 745 | 85.42 | 6.76 | 40.06 | 98.38 | Nucleus |
| Actinidia26414 | *AcShaker27* | 900 | 100.69 | 6.85 | 39.11 | 93.38 | Nucleus |
| Actinidia15691 | *AcShaker28* | 559 | 62.98 | 6.74 | 27.8 | 98.82 | Nucleus |

The phylogenetic tree was constructed using the ML method of MERGA and IQtree, and the results showed a consistent tree topology (Fig. 2). Based on the clustering results, the kiwifruit *Shaker* gene family can be divided into six subfamilies, namely, subfamilies I, II, III, IV, V, and VI. Among them, subfamily VI contained only 13 *Shaker* genes in kiwifruit, indicating that the kiwifruit *AcShaker13*, *AcShaker14*, *AcShaker6*, *AcShaker24*, *AcShaker9*, *AcShaker23*, *AcShaker8*, *AcShaker1*, *AcShaker25*, *AcShaker20*, *AcShaker7*, *AcShaker20*, and *AcShaker4* genes are distantly related to the *Shaker* genes of Arabidopsis. Except for subclade VI, subclade I had the greatest number of *AcShaker* genes, containing nine gene family members, including six in kiwifruit and three in Arabidopsis. Subclade IV contained two genes, *AcShaker22* and *AtKC1*, showing that the kiwifruit A*cShaker22* gene was most closely related to *Arabidopsis* AtKC1. In addition, two, two, and four *AcShaker* family member genes were identified in subclades II, III, and V, respectively.

### Multiple sequence comparison and three-dimensional structure of proteins encoded by the *AcShaker22* and *AtKC1* genes

Multiple alignments of the protein sequences encoded by the *AcShaker22* and *AtKC1* genes showed (Fig. 3A) that the two genes were highly conserved and had high protein sequence similarity, suggesting similar functions. Proteins with structurally alike sequences have conserved three-dimensional structures, and conserved structural domains in different proteins have conserved functions. The tertiary protein structures of *AcShaker22* and *AtKC1* were constructed using SWISS-MODEL software. The results showed (Fig. 3B) that the protein structures of the two genes were highly similar, and the ratios of α-helices, β-sheets, elongated strands, and free coiling were very close to each other. This finding suggested that the structural domains of the two proteins are very similar and have conserved functions.

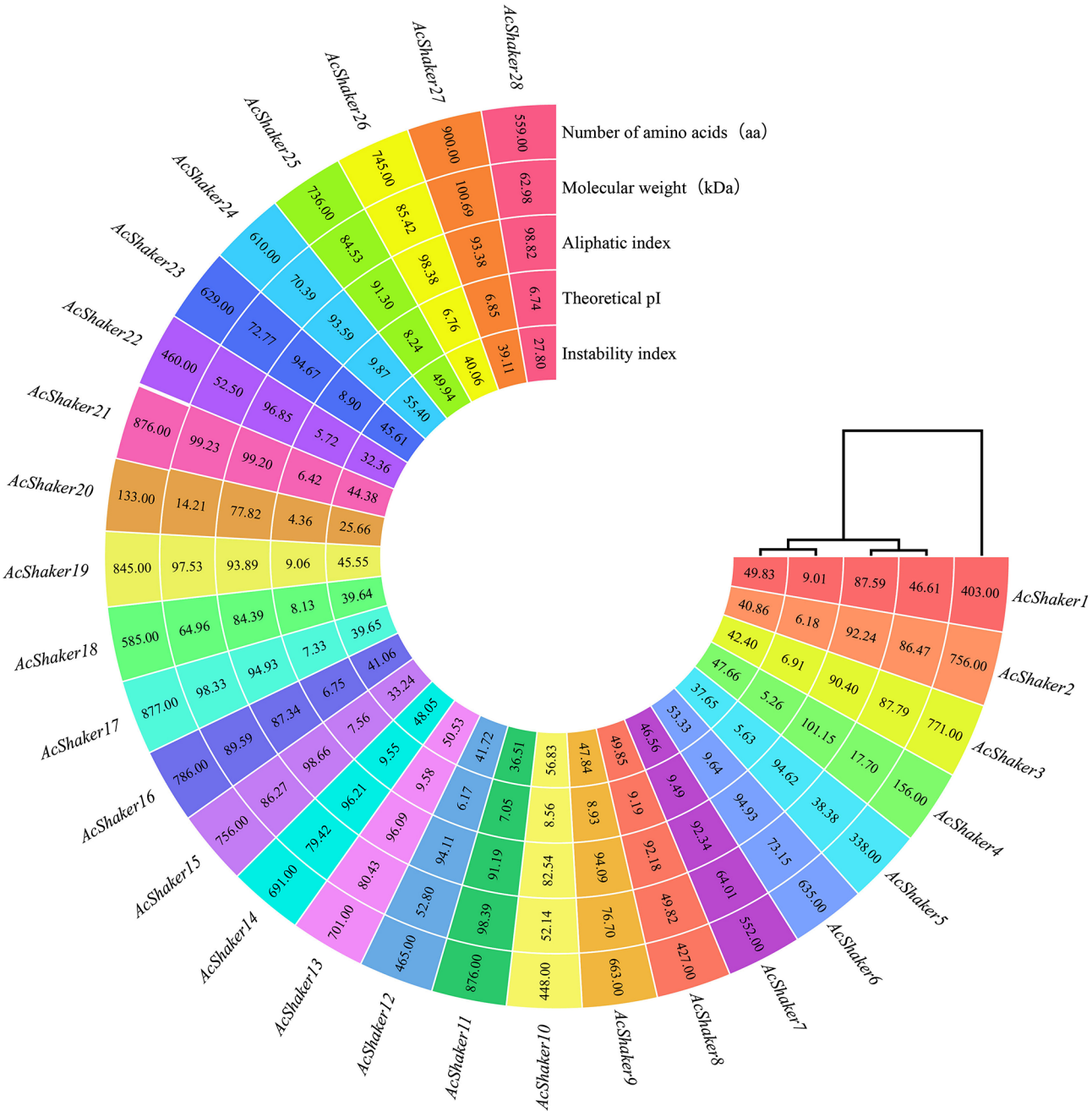


**Fig. 1** Physicochemical property analysis diagram of *AcShaker* genes. The numbers in the heatmap indicate numerical values. Different genes are indicated by different colors. The gene name is indicated by the outermost circle, followed by the number of amino acids (aa), molecular weight (kDa), aliphatic index, theoretical pi, and instability index

### Gene structure, structural domains, and conserved motifs of the kiwifruit *Shaker* gene family

To investigate the sequence characteristics of the *AcShaker* protein, the motif composition of this protein was analyzed in this study using the MEME online tool (Fig. 4B). The results showed that motifs 1, 2, 4, 5, and 10 were highly conserved. However, the same motifs had different positions in different protein sequences, which might be related to the structure and function of this protein. Motif 8 appeared twice in the protein sequences of *AcShaker2*, *AcShaker11*, *AcShaker15*, *AcShaker17*, *AcShaker18*, *AcShaker21*, *AcShaker26*, *AcShaker27*, and *AcShaker28* (Fig. 4A, B), suggesting that subfamily I, II and III *AcShaker* genes may be involved in specific functions. All genes in subfamily II contain eight motifs, and it can be hypothesized that the motif distribution of members of this subfamily is highly conserved. However, even for members of the same subfamily, there were

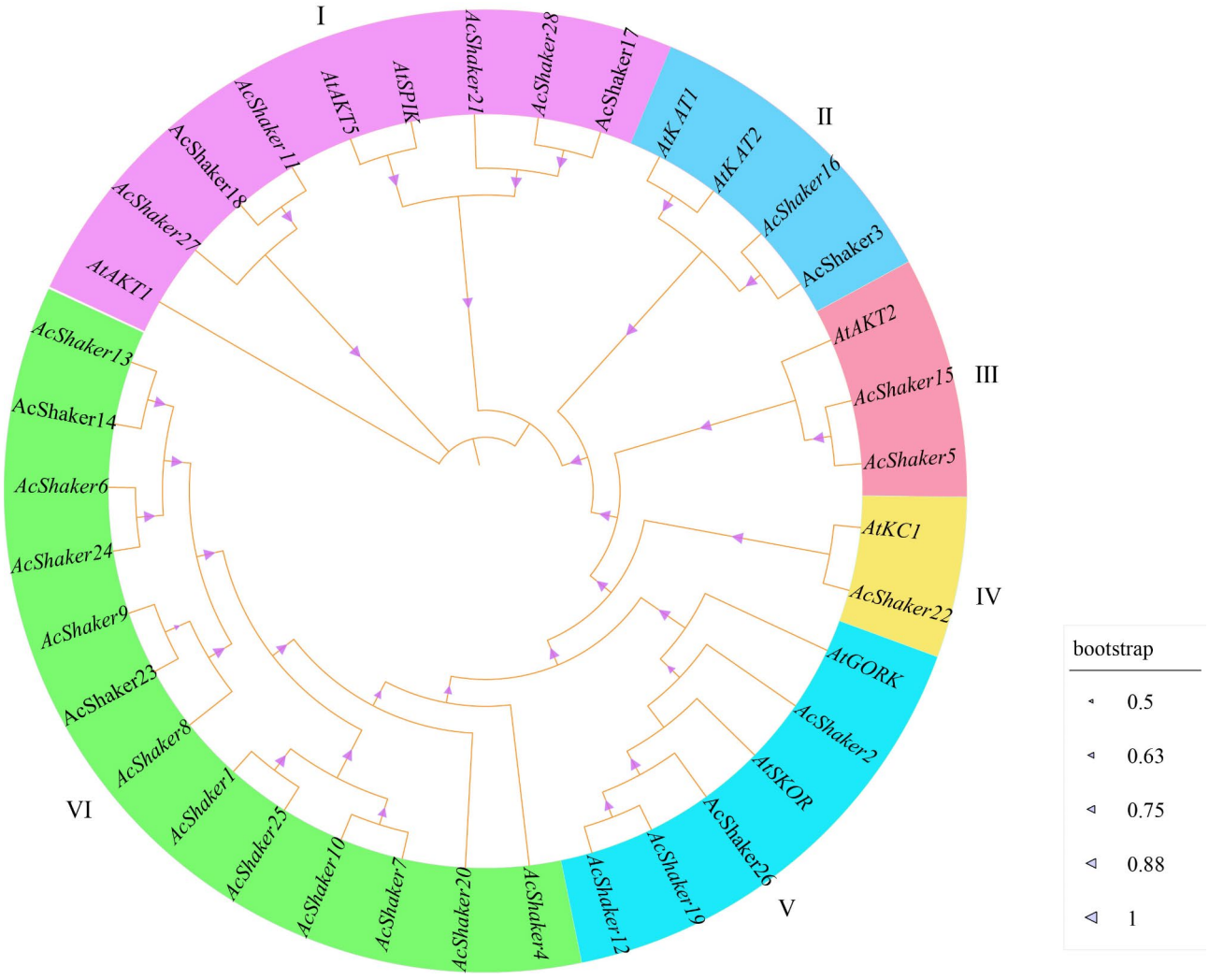


**Fig. 2** Phylogenetic tree of the *Arabidopsis* and kiwifruit *Shaker* gene families. The phylogenetic tree was constructed using the maximum likelihood method with 1000 replicate bootstrap values, with different groupings indicated by different colors

some differences in motif distribution, such as motif 8 appearing twice in the protein sequences of *AcShaker2* and *AcShaker26* in subfamily V (Fig. 4A, B). This may be because differences exist between transcription factor family genes under specific conditions.

Differences in the distribution of conserved motifs within *AcShaker* gene families may also be influenced by gene structure and structural domains. The distribution of gene structure is crucial for studying evolutionary traits within gene families, and 28 *AcShaker* genes were subjected to sequence comparison and analyzed for gene structure based on genome annotation files. The results showed (Fig. 4A, D) that the majority (27) of the 28 kiwifruit *Shaker* gene family members were within 25 kb in length, and the remaining gene (*AcShaker2*) was approximately 55 kb. The number of introns and exons in the kiwifruit *Shaker* gene varied, with the number of introns and exons ranging from 1 to 13 and 2–16, respectively. *AcShaker4* contains only one intron, but *AcShaker19* has 13 introns. In addition, this study revealed that genes with closer relationships have more similar gene structures. For example, in subclade I, three genes, *AcShaker17*, *AcShaker21*, and *AcShaker28*, have the same gene structure, although they are different in length.

The conserved structural domains were also analyzed in this study. The results showed that all 27 *AcShaker* proteins, except *AcShaker20*, had the structural domain of the PLN03192 superfamily, and subclades IV and *AcShaker12*, *AcShaker17*, and *AcShaker19* contained special KHA structural domains (dimerization structural domains of the $K^+$ channel). *AcShaker12* and *AcShaker19* both contain two special structural domains. *AcShaker20* has a special structural domain in the PTZ0032 superfamily. *AcShaker1*, *AcShaker6*, *AcShaker8*, *AcShaker10*, *AcShaker13*, *AcShaker14*, *AcShaker23*, *AcShaker24*, and *AcShaker25* in subfamily VI all have special CAP_ED

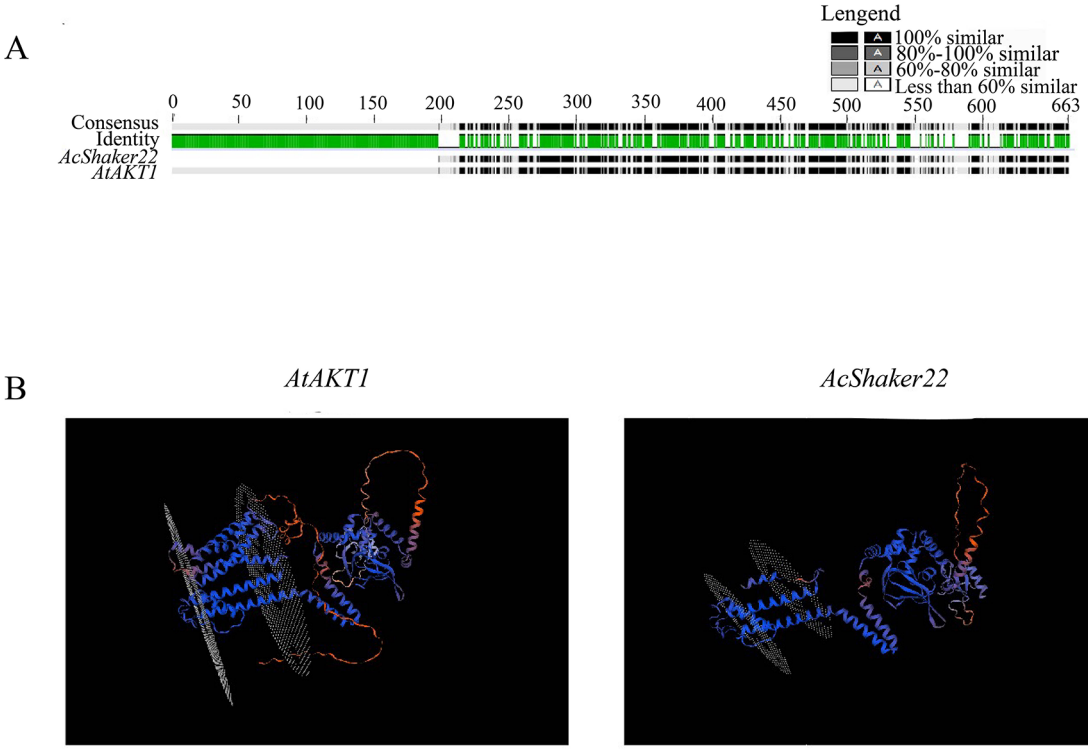


**Fig. 3** Sequence comparison and tertiary structure maps of the *AcShaker22* and AtKC1 proteins. (**A**) Multiple comparisons of protein sequences encoded by the *AcShaker22* and *AtKC1* genes; black and gray shading indicate identical and similar amino acid residues, respectively. (**B**) Three-dimensional structure maps of the AcShaker22 and AtKC1 proteins

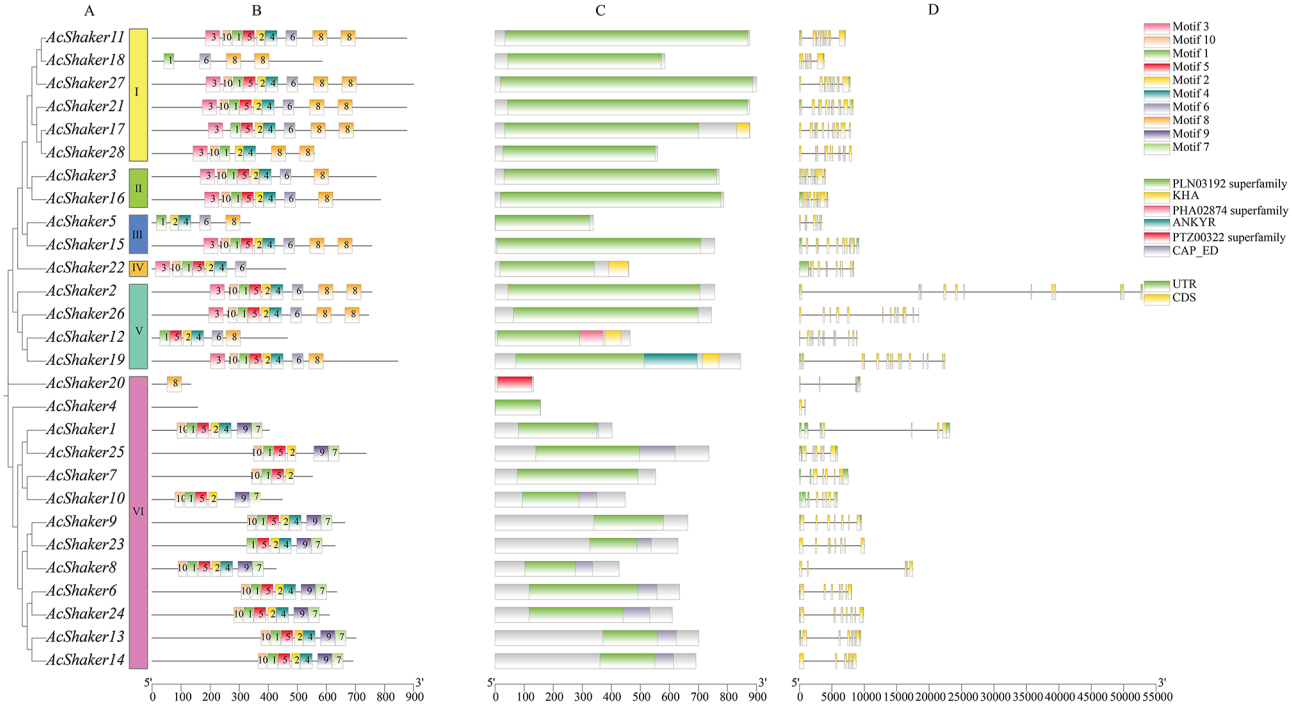


**Fig. 4** Phylogenetic relationships, gene structures, structural domains, and conserved motif distributions of *AcShaker* $K^+$ channel protein family genes. (**A**) Phylogenetic tree analysis of 28 *Shaker* family genes constructed by MERGA. (**B**) Distribution of conserved motifs in *AcShaker*. Motifs are indicated by colored boxes, and black lines indicate the relative length of the proteins. (**C**) Conserved structural domains of *AcShaker* genes. (**D**) The exon-intron structure of the *AcShaker* gene

structural domains (Fig. 4A, C). These findings further verify that regardless of the distribution of conserved motifs, gene structures, or structural domains, there is a certain correlation with phylogenetic relationships, and the closer the evolutionary relationship is, the more similar the sequence features of *AcShaker* gene family members are, and the more identical their structures are.

### Prediction of cis-acting elements of the *AcShaker* gene

To further study the response mechanism of the kiwifruit *Shaker* gene and the response mechanism, 28 promoter cis-acting elements in the 2000 bp sequence upstream of the kiwifruit *Shaker* gene were preprocessed using the online software PlantCARE. The prediction results (Fig. 5, Table S3) revealed a total of 330 promoter cis-acting elements, which could be classified into six main categories: phytohormone response elements (47.58%), environmental stress response elements (22.41%), MYB binding sites (3.64%), protein binding sites (2.12%), light response elements (14.41%) and plant-specific regulatory elements (9.70%). Among the phytohormone response elements, abscisic acid response elements (53) and jasmonic acid response elements (40) accounted for the greatest proportion; among the environmental stress response elements, low-temperature response elements (20) were the most numerous, followed by drought response elements (12). The greater number of drought stress response elements may be related to the fact that $K^+$ can guide stomatal opening and closing and cellular water uptake [54]. In summary, in addition to light response elements, 85.5% of promoter cis-acting elements can regulate gene expression and material metabolism in plants. Promoter cis-acting element analysis suggested that kiwifruit *Shaker* gene family expression may improve kiwifruit adaptation under various adverse conditions, including low-$K^+$ stress.

### Chromosome mapping and replication of the *Shaker* gene in kiwifruit

The results of chromosomal localization (Fig. 6) indicated that the 28 *Shaker* genes of kiwifruit were unevenly distributed on 18 chromosomes. The greatest number of genes were located on chromosomes 1 and 2 (3); an equal number of genes were located on chromosomes 7, 11, 15, 16, 20, 22, and 28 (1); and two genes were located on chromosomes 2, 6, 13, 17, 19, and 26. There was no significant correlation between the number of *Shaker* genes on chromosomes and chromosomes.

Gene tandem duplication and fragment duplication are crucial means of gene family expansion in plants; after multiple duplications, the number of gene family members increases, and plants can better cope with complex environmental changes, including low $K^+$ levels. There are more *AcShaker* genes than *Arabidopsis* genes [32]. To understand the duplication of *AcShaker* family genes in kiwifruit, we performed a gene duplication analysis of 28 *AcShaker* genes (Fig. 4). The results revealed no tandemly duplicated genes, but 13 segmentally duplicated gene pairs were identified. These results suggest that segmental duplications may play a key role in gene duplication

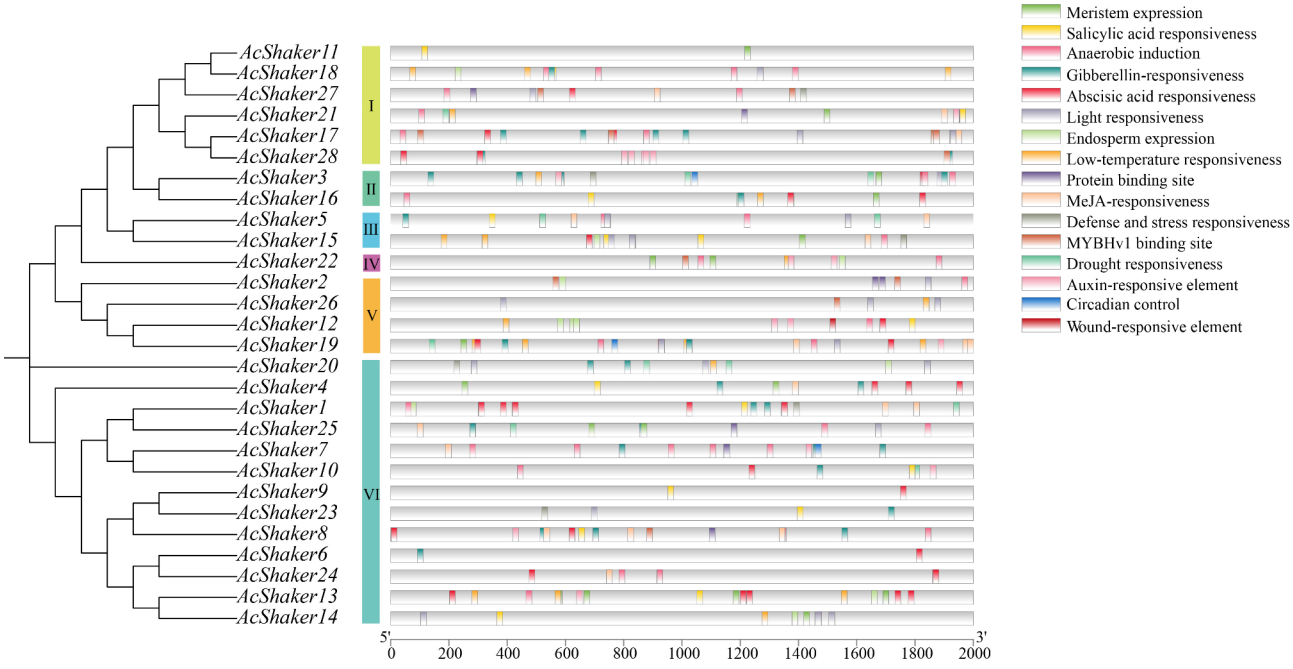


**Fig. 5** Distribution of cis-acting elements in the 2000 bp sequence upstream of the 28 *AcShaker* $K^+$ channel protein family genes, with different cis-acting elements indicated by different colors

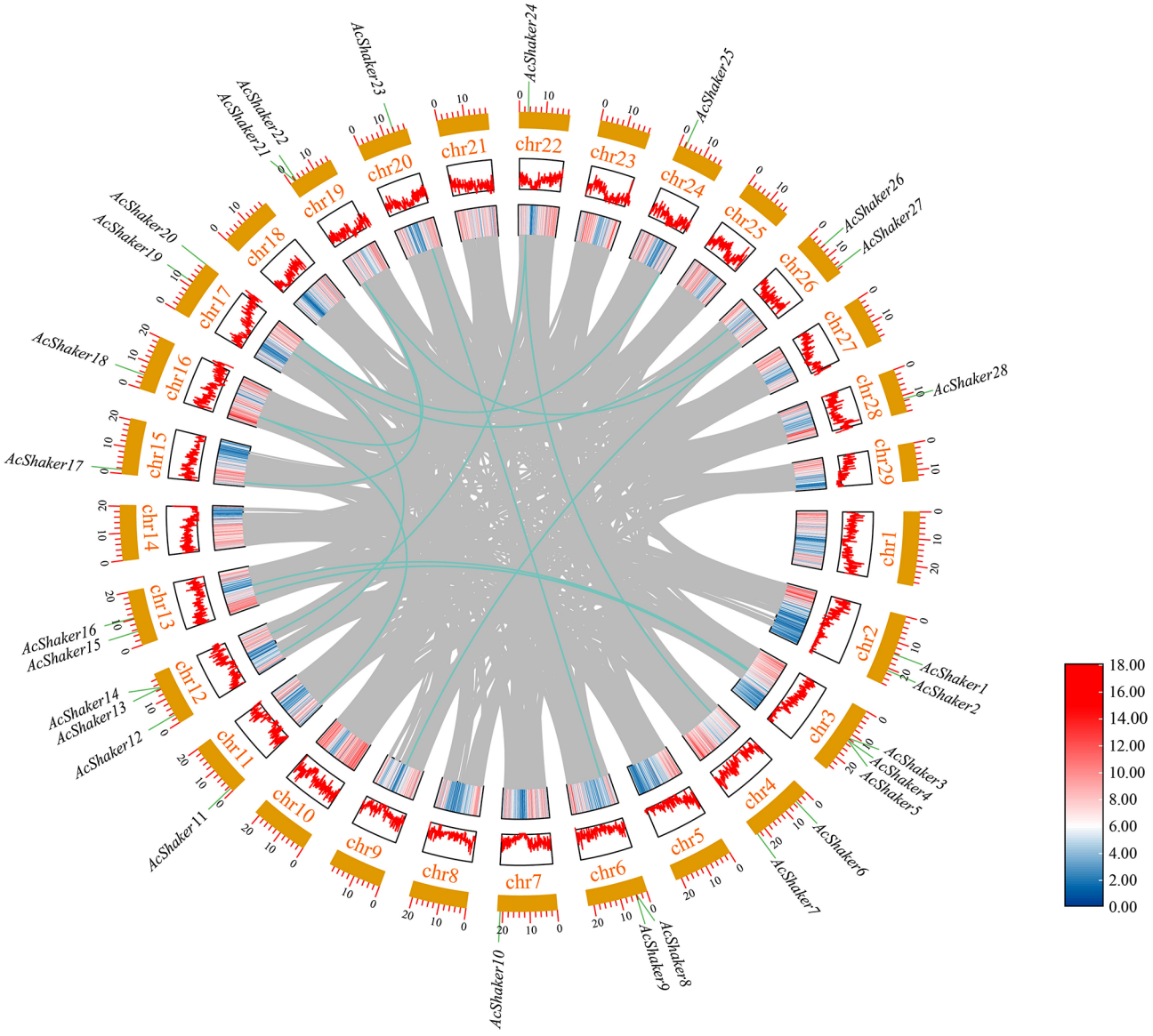


**Fig. 6** Covariance analysis of kiwifruit *AcShaker* genes. The gray lines indicate all duplicated genes; the blue-green lines represent segmentally duplicated *Shaker* gene pairs. The heatmaps and line plots are gene densities, with line densities increasing sequentially from blue to white to red, and the yellow rectangles are chromosomes, with chromosome names shown between each chromosome and gene density

events in the *AcShaker* family, consistent with findings in cabbage [32].

### GO functional enrichment of the *Shaker* genes

To further elucidate the biological functions of *AcShaker* family genes, in this study, the proteins of 28 *AcShaker* genes were annotated for gene functions using the Egg-NOG-MAPPER database and plotted and visualized with the online tool ChiPlot (Fig. 7). The 28 *AcShaker* genes were annotated and assigned to three broad categories, namely, biological process, cellular component, and molecular function. In particular, in terms of biological processes, transmembrane transport, metal cation transport, monoprotic cation transport, inorganic ion transmembrane transport, biomass regulation, and bioregulatory pathways were enriched with more *AcShaker* genes. The modes of $K^+$ transport were transmembrane transport, metal cation transport, and inorganic ion transmembrane transport [55], which suggests that the genes of the *AcShaker* family of genes may enable plants to adapt to the environment by regulating ion transport, including $K^+$ transport, to adapt to adverse environments. All *AcShaker* genes were enriched in membrane and membrane-intrinsic components. Among molecular functions, the number of enriched *AcShaker* genes was greater for monogenic cation transmembrane-transporter protein activity, voltage-gated monogenic cation through rice activity, and inorganic molecular entity

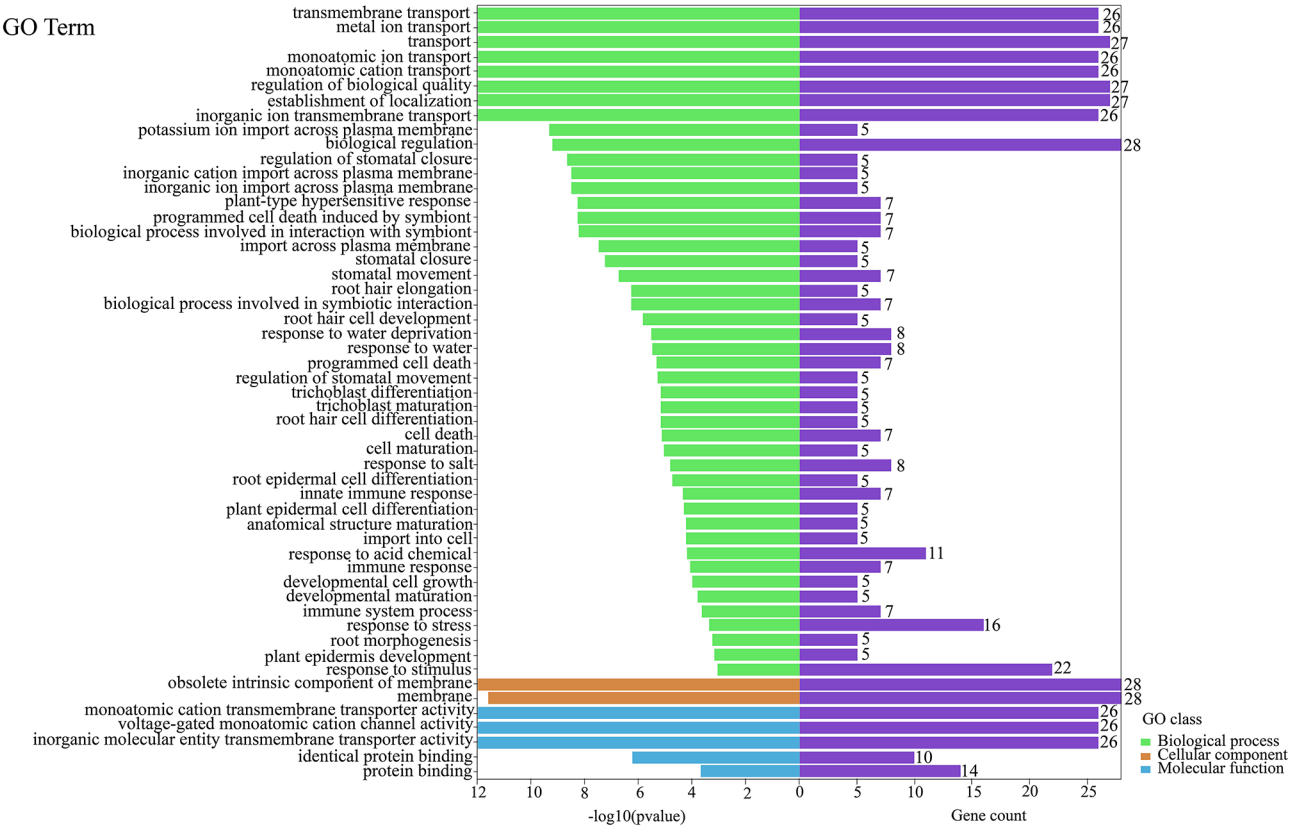


**Fig. 7** GO annotation results for *AcShaker* genes. Biological process, cellular component, molecular function, and gene count are shown in green, orange, blue-green, and purple, respectively. The x-axis indicates the value and number of gene functions, and the y-axis represents the annotation function of the gene

transmembrane transporter activity, indicating that molecular functions play a vital role in the regulation carried out by *AcShaker* family genes. The number of genes enriched in each prime category was significantly greater than 28, suggesting that the same gene may play different roles in different functional entries.

## Response of the *Shaker* gene in Kiwifruit to low-$K^+$ stress and salt stress

### *Determination of low-$K^+$ concentrations and phenotypic observations of leaves and roots*

The uniformly grown histocultured seedlings were connected to media with different $K^+$ concentrations, and their growth was observed every 5 d. First, the weight of the histocultured seedlings in each period was recorded, the growth was calculated and recorded, and the average value was taken every 5 d (Fig. S1, Table S4). Second, the growth results of each period were analyzed by ANOVA using SPSS (Table S5), and the differences in growth characteristics of the group-cultured seedlings were analyzed for each weight (Table S6). Finally, the growth of $K^+$-deficient kiwifruit was analyzed by discriminant analysis (Fig. S2, Tables S7, S8). The results showed that treatment group 5 had the greatest effect on $K^+$ deficiency in 'Hongyang' kiwifruit.

After controlling the length of the roots, the kiwifruit plants were cultured under low-$K^+$ conditions and in MS media for 30 d. The results indicated (Fig. 8) that under low-$K^+$ stress, the kiwifruit leaves turned red, the number of root hairs increased, and heel growth accelerated. For roots and root hairs, the $K^+$-deficient group had many more roots than the control group, and the average root length was approximately twice as long as that of the control group. The data on red leaves, roots, root hairs, and mean root length of CK and T plants (Table S9) were analyzed by ANOVA using SPSS, and the differences were highly significant ($P<0.001$).

## Expression pattern of the *Shaker* $K^+$ protein in kiwifruit under low-$K^+$ stress

In this study, we analyzed the transcriptome data of 'Hongyang' kiwifruit plants after low-K+stress to understand the expression pattern of *AcShaker* genes in 'Hongyang' kiwifruit under low-$K^+$ stress. The results showed (Fig. 9) that all 28 *AcShaker* genes were expressed, with 12 genes showing upregulation and 16 genes showing downregulation. The differential expression of

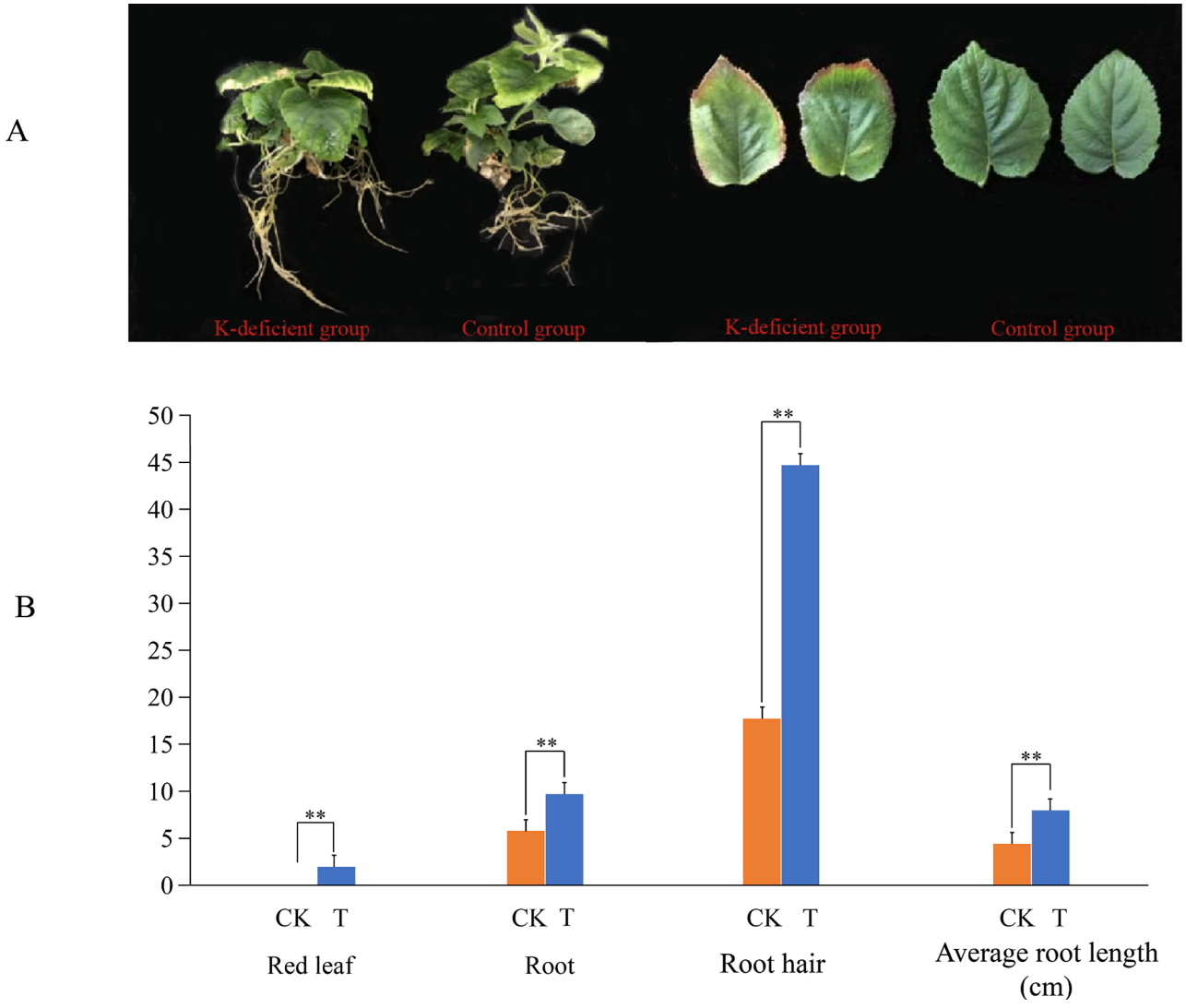


**Fig. 8** Phenotypic observation plots of kiwifruit in $K^+$-deficient and control media. **A**, comparison of kiwifruit roots and leaves cultured in $K^+$-deficient and regular media for 10 d. **B**, mean values of red leaves, roots, root hairs, and root length of kiwifruit plants cultured for 10 d in $K^+$-deficient medium (T) or normal medium (CK). **: $P < 0.01$

three genes (*AcShaker15*, *AcShaker17*, and *AcShaker22*) was significantly varied from that of the control, with p-values less than 0.001. Among the three DEGs, the *AcShaker15* and *AcShaker17* genes were downregulated, and the *AcShaker22* gene was upregulated. There were more downregulated genes with significant differential expression than upregulated genes, which suggests that *AcShaker* genes may negatively regulate the damage caused by low-$K^+$ stress to 'Hongyang', thus improving the ability of plants to resist low-$K^+$ stress.

### qRT-PCR analysis

To verify the accuracy of the transcriptome data, ten genes whose expression significantly differed were selected for qRT-PCR validation. Tables S10 and S11 show that the correlation between the qRT-PCR and RNA-Seq data was high, which confirmed the accuracy of the transcriptome data and verified the reliability of the transcriptome data. The qRT-PCR and RNA-Seq results of three *AcShake* genes (*AcShake15*, *AcShake17*, and *AcShake22*) showed (Fig. 10) that the correlation between the qRT-PCR and RNA-Seq expression of the three AcShake genes was high, indicating that the *AcShake15*, *AcShake17*, and *AcShake22* genes play crucial regulatory roles in the low-$K^+$ stress response.

### Expression pattern of the *Shaker* gene in kiwifruit under salt stress

To understand the expression pattern of *AcShaker* genes in kiwifruit under salt stress, transcriptome data from kiwifruit plants after salt stress were analyzed in this study. The results showed (Fig. 11) that there were 28

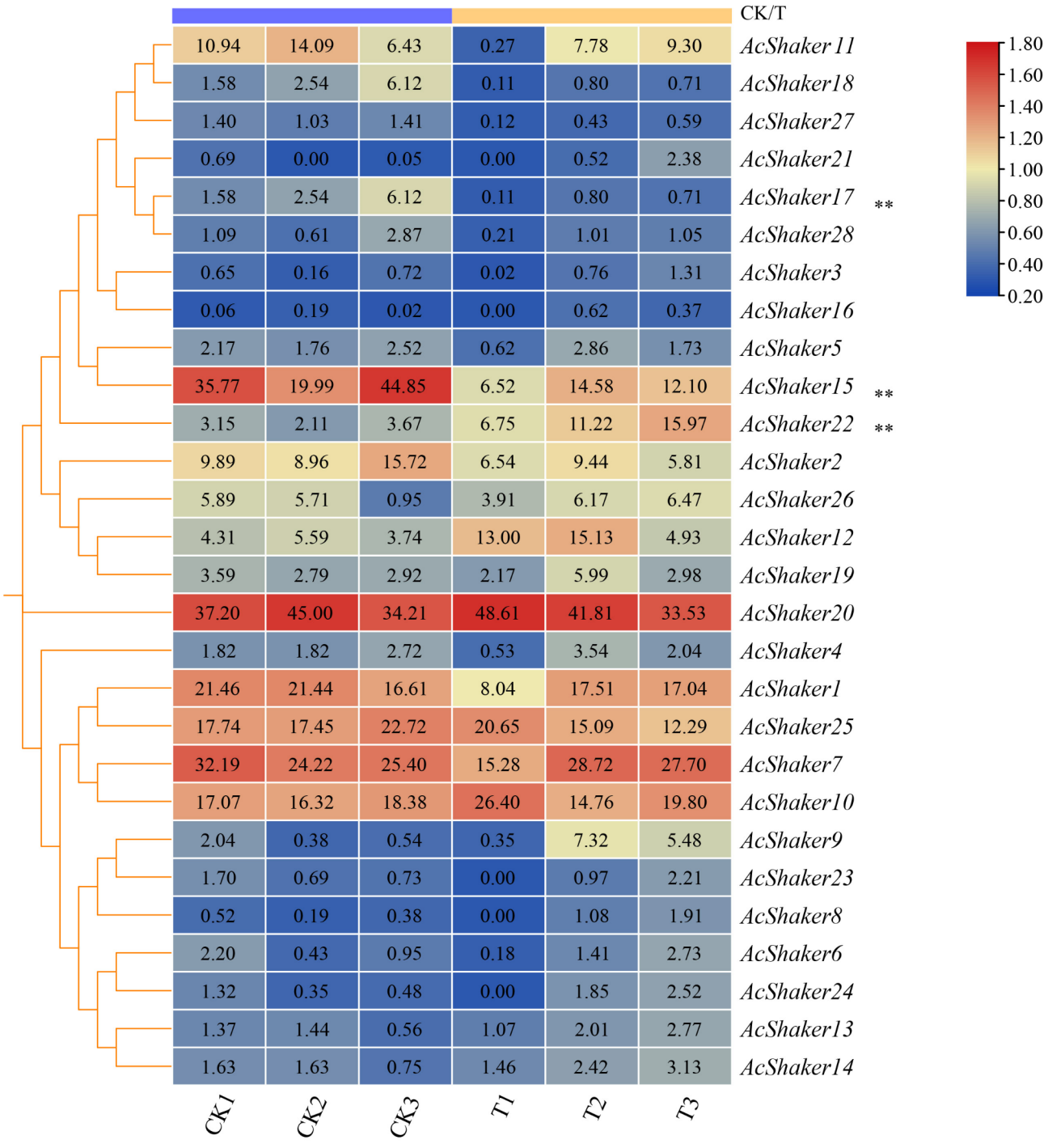


**Fig. 9** Heatmap of the expression profiles of 28 *AcShaker* genes under low-$K^+$ stress. The various colored boxes indicate different $\log_2$ (FPKM) values; the expression gradually increased from blue to yellow to red. CK is the control group, and T is the treatment group; **: $P < 0.01$

*AcShaker*-expressed genes in both groups of kiwifruit under salt stress. Seventeen genes were downregulated, and 11 were upregulated in the T1 treatment group. Compared with those in the control group, six genes were significantly differentially expressed, among which the *AcShaker9* and *AcShaker27* genes were upregulated, and the *AcShaker11*, *AcShaker18*, *AcShaker21*, and *AcShaker24* genes were downregulated. In the T2 treatment group, 15 genes were downregulated, and 13 were upregulated. Both genes (*AcShaker11* and *AcShaker18*) showed significant differential expression compared to the control group. In the T3 treatment group, 11

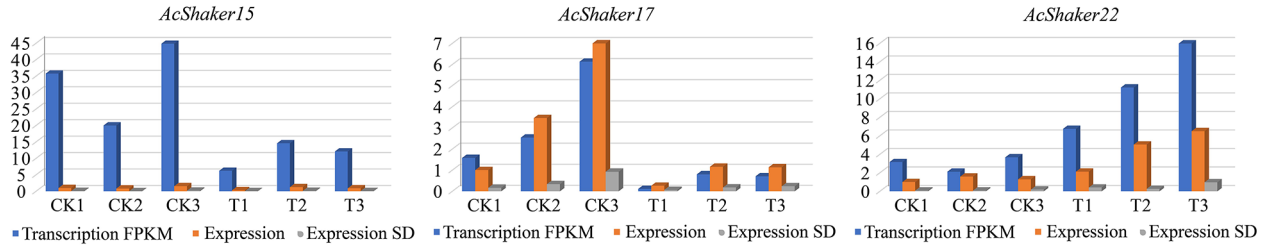


**Fig. 10** Plot of qRT-PCR versus RNA-Seq expression of three differentially expressed *AcShaker* genes (*AcShaker15*, *AcShaker17*, and *AcShaker22*) under low-$K^+$ stress. Blue: RNA-Seq data; orange: qRT-PCR data; gray: standard deviation of the qRT-PCR data. r: correlation coefficient of qRT-PCR and RNA-Seq expression. CK1, CK2, and CK3 were used as the controls, and T1, T2, and T3 were used as treatments

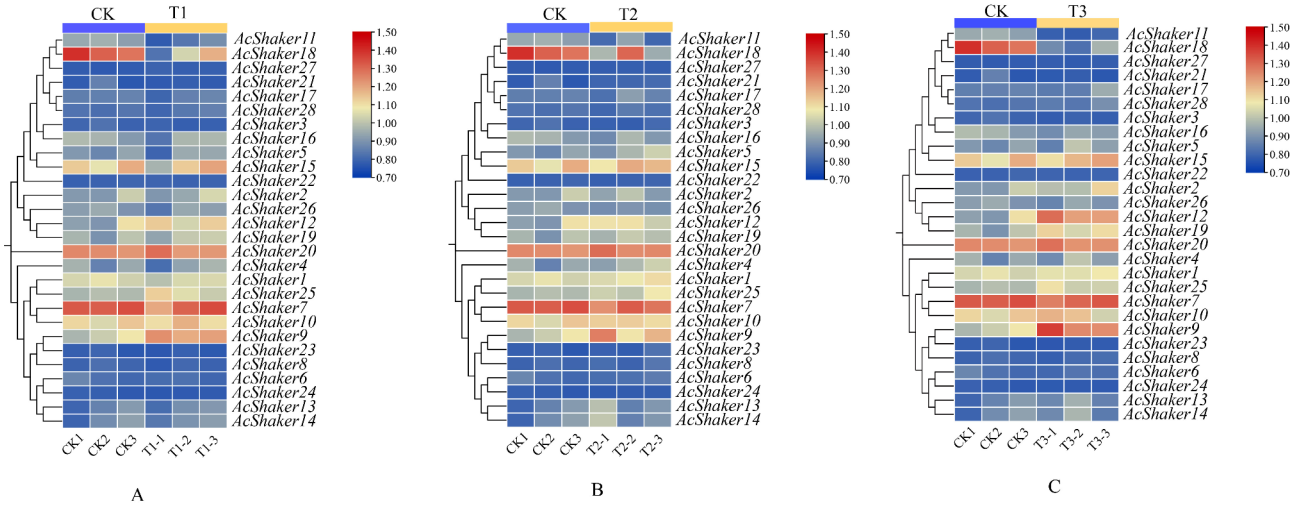


**Fig. 11** Heatmap of the expression profiles of 28 *AcShaker* genes under salt stress. **A**, **B**, and **C** show the gene expression heatmaps of the T1, T2, and T3 groups and the CK comparison. The various colored boxes indicate different log2 (FPKM) values; the expression gradually increased from blue to yellow to red. CK is the control group, and T is the treatment group

genes were downregulated, and 17 were upregulated. Eight genes were significantly differentially expressed compared to those in the control group, among which the *AcShaker9*, *AcShaker12*, and *AcShaker19* genes were upregulated, and the *AcShaker11*, *AcShaker18*, *AcShaker21*, *AcShaker23*, and *AcShaker24* genes were downregulated. The *AcShaker11* and *AcShaker18* genes differed significantly among the three groups of salt treatments, and all were downregulated. The number of downregulated genes with significant differential expression was greater than that of upregulated genes, suggesting that *AcShaker* genes may enhance plant resistance to salt stress by negatively regulating the damage caused by salt stress in kiwifruit.

## Discussion

*Shaker* $K^+$ channels are typical $K^+$ channels involved in $K^+$ uptake and stress resistance in higher plants [36]. Shaker $K^+$ channel proteins in plants are highly similar in structure to *Shaker* $K^+$ proteins in Drosophila [56]. In recent years, *Shaker* $K^+$ channels have been categorized into three main types, namely, inwardly rectifying, outwardly rectifying, and weakly rectifying $K^+$ channels, based on voltage dependence and the direction of $K^+$ transmembrane transport [57]. In this study, 28 *Shaker* genes were identified in 'Hongyang' kiwifruit. Phylogenetic analysis revealed that 13 genes, including *AcShaker6*, *AcShaker13*, and *AcShaker14*, did not cluster with *AtShaker* genes, suggesting unique functions. The *Shaker* genes of kiwifruit can be divided into six subfamilies (Fig. 2). Among them, the *AtAKT1* gene belongs to subfamily I, and it has been shown that *AtAKT1* plays a vital role in $K^+$ uptake, tolerance to low-$K^+$ stress and tolerance to high salt stress [29]. It is hypothesized that the genes in clade I have similar functions. This classification was more apparent in the comprehensive analysis of conserved motifs, gene structures, and structural domains. According to the conserved motif analysis, similar genes were clustered in almost the same subfamily, and there were multiple motifs in specific proteins, which implies that they may have exceptional functions [36].

Structural analyses of the genes revealed that the number of introns in the kiwifruit *Shaker* gene varied considerably, with the number of introns ranging from 1 to

13 (Fig. 4). This gene was similar to the *Shaker* genes in cabbage [32], pear [34], sweet potato [35], soybean [36], and woolly cotton [28]. Many variations in the number of introns in the *Shaker* genes of kiwifruit may be due to chromosomal variation resulting from paleopolyploid events [58], which may have led to the diversity of gene functions. The clustering of the phylogenetic tree was highly similar to the structural features of the conserved motifs, gene structures, and structural domains, further suggesting that genes with similar evolutionary processes may also have similar functions, thus contributing to screening for *Shaker* genes with similar functions. For example, the overexpression of *OsAKT1* in rice increased the $K^+$ content in tissues and improved drought tolerance [59]. Overexpression of *GmAKT1* in *A. thaliana* increased root length and potassium concentration under drought and salt stress, suggesting that *GmAKT1* plays a role in the response of soybean plants to these stresses [36]. Overexpression of *HvAKT1* in barley increased the $K^+$ content in tissues and improved plant tolerance to drought [60]. *The* roots of sweet potato plants overexpressing IbAKT1 showed greater $K^+$ influx than adventitious roots and lower $K^+$ efflux than adventitious roots under $K^+$ deficiency stress, indicating that *IbAKT1* may play a vital role in the regulation of $K^+$ deficiency tolerance in sweet potato plants [35]. It can be hypothesized that *AcShaker* genes play an important role in abiotic stress regulation, especially under abiotic stresses, including $K^+$ deficiency stress [61, 62]. This finding was further confirmed by expression profiling in this study.

Promoter homeopathic action elements play vital roles in regulating transcription and gene expression [63–65]. In this study, a large number of homeostatic elements related to kiwifruit resistance, such as ABA response elements, MeJA response elements, SA response elements, and hypoxia-induced response elements, were identified in the 2000 bp sequence upstream of the kiwifruit *Shaker* gene (Fig. 5). Numerous previous studies have shown that both ABA [66, 67] and MeJA [68–70] can stimulate the expression of plant defense genes and induce chemical defenses and some physiological and functional stress responses. Anaerobic induction [71] enhances plant tolerance to hypoxia, confers the ability to adapt to survival under hypoxic conditions, and effectively improves plant stress tolerance. In conclusion, from the results of homologous promoter role element prediction, the kiwifruit vibrational gene family plays a vital role in kiwifruit resistance to various stresses. Moreover, the GO enrichment analysis in this study revealed that transmembrane transport, inorganic ion transmembrane transport, and bioregulatory pathways were enriched with a greater number of *AcShaker* genes (Fig. 7), suggesting that genes in the *AcShaker* gene family can adapt plants to adverse environments by regulating ion transport [32, 34, 57].

Many studies have shown that gene duplication is the prime mode of gene amplification and one of the main molecular mechanisms by which genes evolve to produce genes with new functions [72, 73]. We analyzed the gene duplication events occurring in the *Shaker* gene family of kiwifruit (Fig. 5). We detected 13 pairs of gene duplications in 28 *Shaker* genes, all of which were segmental duplications without tandem duplications, indicating that gene duplication events are also vital means of expanding the *Shaker* gene family in kiwifruit. In addition, the greatest number of *Shaker* gene duplications occurred on chromosomes 17 and 26, along with a relatively high number of genes chromosomally localized to chromosomes 17 and 26, suggesting that kiwifruit chromosomes 17 and 26 may contain relatively vital kiwifruit gene resources. The efficiency of $K^+$ uptake may increase after multiple replication events. The replication results suggest that there should be a polyploidization event in kiwifruit, thus confirming the findings of Shi et al. [58].

In this study, 'Hongyang' kiwifruit showed the most severe deficiency in seedlings in MS media with an $NH_4NO_3$ concentration of 600 mg/L and a $KNO_3$ concentration of 100 mg/L (Fig. S1 and S2). Although the seedlings could grow, the growth quality was almost negative. The edges of the leaves of the seedlings of this combination were red or brown at the later stage, which was in agreement with the results of the study conducted by Lin et al. [74], and kiwifruit was at a $K^+$-deficient level. It is reasonable to use this combination for subsequent transcriptome analysis and consequent analysis of the expression profiles of *Shaker* gene family members.

Observations of leaf and root phenotypes after 30 d of $K^+$ deficiency revealed a generalized reddening of leaf margins, a significant increase in the number of roots and root hairs, and a longer root length in $K^+$-deficient plants than in controls (Fig. 8). These are typical $K^+$ deficiency phenomena in plants. In rice, when subjected to low-$K^+$ stress, leaves become darker in color, and the appearance of old leaves resembles burnt symptoms [75]. In kiwifruit, the symptoms of $K^+$ deficiency in the field were greenish leaves and slight wilting of the leaf margins of old leaves, which were consistent with the results of this experiment [76]. According to the results of this study, the number of roots and root hairs and the length of the roots of 'Hongyang' kiwifruit increased significantly after $K^+$ deficiency compared to those in the control group; therefore, 'Hongyang' kiwifruit is a plant with high $K^+$ uptake efficiency.

To further elucidate the biological functions of *Shaker* genes and the principles of their regulation, we analyzed the expression patterns of the *Shaker* gene family in conjunction with the transcriptome of kiwifruit under low-$K^+$ stress. The results showed that all 28

*Shaker* genes could be expressed under low-$K^+$ stress with high transcript levels (Fig. 9), among which three genes were differentially expressed at significantly different levels. Among the three DEGs, the *AcShaker15* and *AcShaker17* genes were phenotypically downregulated, and the *AcShaker22* gene was upregulated. The three AcShake DEGs were subjected to qRT-PCR verification, and the correlation between the results of qRT-PCR and transcriptome sequencing was high (Fig. 10), which confirmed the accuracy of the transcriptome data and verified the reliability of the transcriptome data with the DEGs. The *AcShaker22* gene belongs to subfamily IV (*KC1*) (Fig. 2), a subunit of the K-channel protein family *Shaker*, and it is primarily expressed in the roots. In *A. thaliana*, the *AtKC1* gene is localized in root hairs as a channel to regulate $K^+$ uptake by roots [77]. The kiwifruit *AcShaker22* gene can regulate the root uptake of $K^+$. In 2002, Birgit investigated the role of the *AtKC1* gene in *A. thaliana* roots and demonstrated that the *AtKC1/AKT1* tetramer, formed by *AtKC1* and *AKT1*, was able to regulate the uptake of K in root hairs [78]. The *AcShaker15* and *AcShaker17* genes belonging to subgroup III (*AKT2*) and subgroup I (*AKT1*) were downregulated, whereas *AKT1* and *AKT2* exhibited similar $K^+$ penetration in leaf sclerotial cells [35].

In this study, the phylogenetic tree grouped the *AtKC1* gene of *A. thaliana* into the same (IV) subclade as the *AcShaker22* gene of kiwifruit and the *AtAKT1* gene and *Shaker17* into the same (I) subclade (Fig. 2), suggesting that they may have similar gene functions. Sequence comparison and protein three-site structure prediction revealed (Fig. 3) that *AcShaker22* and *AtKC1* have similar protein sequences and similar protein structures, and it is hypothesized that *AcShaker22* and *AtKC1* have similar functions. Posttranslational regulation is a vital regulatory mechanism for $K^+$ channel activity in plant cells [78–80]. Transcriptional regulation of $K^+$ transporters is another important mechanism for plants to cope with environmental stresses, and $K^+$ deprivation may induce the transcription of some $K^+$ transporters [81, 82]. Wang et al. demonstrated that the *AKT1* gene in *Agrobacterium dalianensis* was negatively regulated by low-$K^+$ stress [77]. The *AtKC1* gene, a regulator of *AKT1*, negatively regulates the activity of *AKT1* under low-$K^+$ stress.

Moreover, *AtKT1* belongs to a subunit of the *A. thaliana Shaker* family of inwardly rectifying channels [34]. Under low-$K^+$ stress (Fig. 9), the *AcShaeker22* and *AcShaker17* genes were significantly expressed in kiwifruit; the *AcShaeker22* gene was upregulated, and the *AcShaeker17* gene was downregulated. These findings suggest that the kiwifruit *AcShaeker22* and *AcShaeke17* genes and the *A. thaliana AtKC1* gene may be regulated similarly to *AtAKT1* (Fig. 12). When kiwifruit perceives low-$K^+$ stress, the transcript level of *AcShake*r may

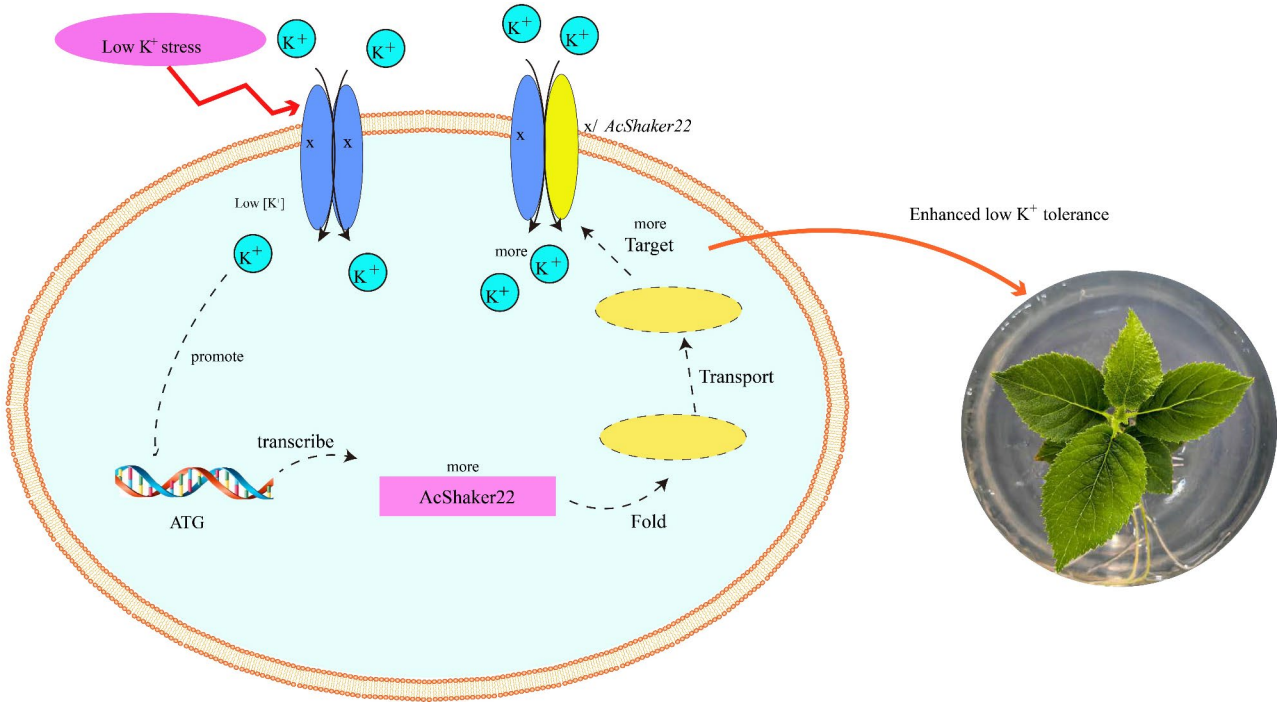


**Fig. 12** Schematic model of the mechanism by which *AcShaker22* regulates $K^+$ channels. x indicates the inwardly rectifying channel subunit (*AcShaker17*) of the kiwifruit *Shaker* family. This is a schematic model of the *AcShaker22* gene mechanism based on a model of the *AtAKT1* gene. When the external $K^+$ concentration is low, the intracellular $K^+$ concentration in the plant also becomes low, which may induce transcription of the *AcShaker22*, thereby increasing the rate of $K^+$ uptake and enhancing the plant's tolerance to low $K^+$

increase. It is hypothesized that the *AcShaker22* gene product may interact with other *Shaker* $K^+$ channel subunits, such as the *AcShaker17* gene product. Thus, it may regulate $K^+$ uptake and transport in kiwifruit and contribute to adaptation to environmental changes. However, further studies and functional analyses (e.g., heterologous expression of *AcShaker22* in yeast or Arabidopsis) are needed to better understand the role of the *AcShaker22* gene in response to changes in $K^+$ concentration.

It has been suggested that potassium and sodium ion channels are associated. In this study, nine *AcShaker* genes were significantly differentially expressed under salt stress (Fig. 11). Four of these genes were upregulated (*AcShaker9*, *12*, *19*, and *27*), and five were downregulated (*AcShaker11*, *18*, *21*, *23*, and *24*). The isotropic bidirectional transport of potassium and sodium ions contributes to the maintenance of intracellular $Na^+$/$K^+$ homeostasis, which may play a crucial role in the mechanism of salt tolerance in sugar-leaf plants [83]. The *AcShaker12* and *AcShaker19* genes are in the same subclade V as *SKOR* in *A. thaliana*, suggesting that *AcShaker12* and *AcShaker19* are closely related to *AtSKOR*. The salt-stressed outwardly rectifying $K^+$ channel protein SKOR may be the only *Shaker* $K^+$ channel that plays a role in $K^+$ secretion from xylem sap. Continued accumulation of $Na^+$ in xylem cells causes depolarization of the plasma membrane of thin-walled xylem cells, which activates its activity and the transport of $K^+$ from the xylem to the above-ground parts [84], and it was inferred that the *AcShaker12* and *AcShaker19* genes may have the same function. In conclusion, based on the transcriptional data, kiwifruit *Shaker* genes may play a crucial role in the response of kiwifruit to abiotic stresses such as low-$K^+$ stress and salt stress.

## Conclusion

Twenty-eight *AcShaker* genes were identified from the kiwifruit genome and classified into six subfamilies by phylogenetic analysis. All 28 *AcShaker* genes were found to be expressed in the transcriptome data under both salt stress and low-$K^+$ stress. The three salt stress transcriptome datasets showed that the expression levels of *AcShaker11* and *AcShaker18* varied significantly relative to control conditions. Both genes appeared to be downregulated, suggesting that the *AcShaker* gene may negatively regulate plant injury caused by salt stress. The transcriptome data of plants subjected to low-$K^+$ stress showed significant differential expression of three *AcShaker* genes compared with the control. The qRT-PCR results were strongly correlated with the transcriptome data, indicating that the transcriptome data are reliable. Among these genes, *AcShaker22* expression was differentially and significantly upregulated under low-$K^+$ stress and could be a candidate gene for breeding new low-$K^+$-resistant kiwifruit varieties. Our results on *AcShaker* genes could be utilized in developing transgenic kiwifruit plants that are tolerant to abiotic stress and more efficient at $K^+$ uptake.

### Abbreviations

| | |
|---|---|
| ABA | Abscisic acid |
| *A. Chinensis* | *Actinidia chinensis* |
| *A. Thaliana* | *Arabidopsis thaliana* |
| cDNA | Complementary DNA |
| Chr | Chromosome |
| $CO_2$ | Carbon dioxide |
| d | Day |
| DEGs | Differentially expressed genes |
| FDR | False discovery rate |
| FPKM | Fragments per kilobase per million |
| GA | Gibberellin |
| GO | Gene Ontology |
| h | Hour |
| HMM | Hidden Markov model |
| K | Potassium |
| $K^+$ | Potassium ion |
| KGD | Kiwifruit Genome Database |
| MeJA | Methyl jasmonate |
| ML | Maximum likelihood |
| pI | Isoelectric point |
| qRT-PCR | Quantitative real-time polymerase chain reaction |
| RNA-Seq | RNA sequencing |
| VC | Vitamins |

## Supplementary Information

The online version contains supplementary material available at https://doi.org/10.1186/s12870-024-05555-x.

Supplementary Material 1

### Acknowledgements

The authors thank Prof. Deqiang Zhang, Beijing Forestry University, for his critical reading.

### Author contributions

YQ Z conceived and designed the study and wrote the original manuscript. ZM Z, K Z, L Z and XY Y performed transcriptome and gene expression analyses and assisted with experiments. T Y, K W, XL L and CY C assisted with sampling and fieldwork. XZ L and HY Z reviewed and edited the manuscript. Supervision, HY Z; project management, XZ L; funding obtained, HY Z. All authors have read and agreed to the published version of the manuscript.

### Funding

The study is supported by the Agricultural Joint Key Projects in Yunnan Province (202301BD070001-003), Rural Revitalization Science and Technology Project-Rural Revitalization Industry Key Technology Integration Demonstration Project (202304BP090005), Yunnan Academician (Expert) Workstation Project (202305AF150020), and the National Natural Science Foundation of China (Grant No. 31760450).

### Data availability

All the data generated or analyzed in this study are included in this article. Kiwifruit genome annotation files can be accessed at http://kiwifruitgenome.org/. RNA-Seq data under low-$K^+$ stress can be found with the following registration numbers: PRJNA1021346, the login link is https://submit.ncbi.nlm.nih.gov/subs/sra/SUB13862819. RNA-Seq data under salt stress can be found. The registration number is PRJNA1021945, and the login link is https://submit.ncbi.nlm.nih.gov/subs/sra/SUB13862895. The RNA-Seq data are publicly available at the National Center for Biotechnology Information. The other data presented in this study are available in the Supplementary Materials.

## Declarations

**Ethics approval and consent to participate**
This study did not include human or animal subjects.

**Statement on guidelines**
All experimental studies and experimental materials involved in this research were in full compliance with relevant institutional, national, and international guidelines and legislation.

**Disclosure statement**
No potential conflicts of interest were reported by the authors.

**Consent for publication**
Not applicable.

**Competing interests**
The authors declare no competing interests.

**Author details**
[1]Key Laboratory for Forest Resources Conservation and Utilization in the Southwest Mountains of China, Ministry of Education, Southwest Forestry University, Kunming, China
[2]Key Laboratory of Biodiversity Conservation in Southwest China, National Forest and Grassland Administration, Southwest Forestry University, Kunming 650224, Yunnan Province, China

Received: 24 October 2023 / Accepted: 29 August 2024
Published online: 06 September 2024

**References**

1. Wang R, Shu P, Zhang C, Zhang J, Chen Y, Zhang Y, Du K, Xie Y, Li M, Ma T, Zhang Y, Li Z, Grierson D, Pirrello J, Chen K, Bouzayen M, Zhang B, Liu M. Integrative analyses of metabolome and genome-wide transcriptome reveal the regulatory network governing flavor formation in kiwifruit (*Actinidia chinensis*). New Phytol. 2022;233(1):373–89. https://doi.org/10.1111/nph.17618. Epub 2021 Aug 4. PMID: 34255862.
2. Salazar JA, Vergara-Pulgar C, Jorquera C, Zapata P, Ruiz D, Martínez-Gómez P, Infante R, Meneses C. De novo transcriptome sequencing in kiwifruit (*Actinidia chinensis* var. *deliciosa* (A Chev) Liang et Ferguson) and development of tissue-Specific transcriptomic resources[J]. Agronomy, 2021(5).doi:https://doi.org/10.3390/AGRONOMY11050919
3. Han X, Zhang Y, Zhang Q, Ma N, Liu X, Tao W, Lou Z, Zhong C, Deng XW, Li D, He H. Two haplotype-resolved, gap-free genome assemblies for *Actinidia Latifolia* and *Actinidia chinensis* shed light on the regulatory mechanisms of vitamin C and sucrose metabolism in kiwifruit. Mol Plant. 2023;16(2):452–70. Epub 2022 Dec 31. PMID: 36588343.
4. Zheng Y, Su L, Tan J, Dong F. *Actinidia chinensis* Planch Root extract suppresses the growth and metastasis of hypopharyngeal carcinoma by inhibiting E2F transcription factor 1-mediated MNX1 antisense RNA 1. Bioengineered. 2022;13(3):4911–22. PMID: 35152841; PMCID: PMC8973797.
5. Zhang G, Bai B, Xu M, Liu Y, Wu Y, Zhao L. Advances in and prospects for *Actinidia* viruses. Plant Dis. 2022;106(5):1321–1329. https://doi.org/10.1094/PDIS-10-21-2270-FE. Epub 2022 Apr 11. PMID: 34941370.
6. Zhao L, Yang W, Zhang Y, Wu Z, Wang QC, Wu Y. Occurrence and molecular variability of kiwifruit viruses in *Actinidia deliciosa* 'Xuxiang' in the Shaanxi Province of China. Plant Dis. 2019;103(6):1309–18. https://doi.org/10.1094/PDIS-09-18-1570-RE. Epub 2019 Mar 25. PMID: 30907694.
7. Zhang JY, Pan DL, Jia ZH, Wang T, Wang G, Guo ZR. Chlorophyll, carotenoid and vitamin C metabolism regulation in *Actinidia chinensis* 'Hongyang' outer pericarp during fruit development. PLoS ONE. 2018;13(3):e0194835. https://doi.org/10.1371/journal.pone.0194835. PMID: 29579114; PMCID: PMC5868826.
8. Johnson R, Vishwakarma K, Hossen MS, Kumar V, Shackira AM, Puthur JT, Abdi G, Sarraf M, Hasanuzzaman M. Potassium in plants: growth regulation, signaling, and environmental stress tolerance. Plant Physiol Biochem. 2022;172:56–69. Epub 2022 Jan 7. PMID: 35032888.
9. Ankit A, Singh A, Kumar S, Singh A. Morphophysiological and transcriptome analysis reveal that reprogramming of metabolism, phytohormones and root development pathways governs the potassium ($K^+$) deficiency response in two contrasting chickpea cultivars. Front Plant Sci. 2023;13:1054821. https://doi.org/10.3389/fpls.2022.1054821. PMID: 36714783; PMCID: PMC9875034.
10. Gohara DW, Di Cera E. Molecular mechanisms of enzyme activation by monovalent cations. J Biol Chem. 2016;291(40):20840–8. https://doi.org/10.1074/jbc.R116.737833. Epub 2016 Jul 26. PMID: 27462078; PMCID: PMC5076497.
11. Lotfi R, Abbasi A, Kalaji HM, Eskandari I, Sedghieh V, Khorsandi H, Sadeghian N, Yadav S, Rastogi A. The role of potassium on drought resistance of winter wheat cultivars under cold dryland conditions: probed by chlorophyll a fluorescence. Plant Physiol Biochem. 2022;182:45–54. Epub 2022 Apr 14. PMID: 35462197.
12. Kaiser WM, Urbach W, Gimmler H. The role of monovalent cations for photosynthesis of isolated intact chloroplasts. Planta. 1980;149(2):170-5. https://doi.org/10.1007/BF00380879. PMID: 24306249.
13. Pier PA, Berkowitz GA. Modulation of water stress effects on photosynthesis by altered leaf k. Plant Physiol. 1987;85(3):655–61. https://doi.org/10.1104/pp.85.3.655. PMID: 16665755; PMCID: PMC1054317.
14. Fontana JE, Wang G, Sun R, Xue H, Li Q, Liu J, Davis KE, Thornburg TE, Zhang B, Zhang Z, Pan X. Impact of potassium deficiency on cotton growth, development and potential microRNA-mediated mechanism. Plant Physiol Biochem. 2020;153:72–80. Epub 2020 May 25. PMID: 32480238.
15. Naciri R, Lahrir M, Benadis C, Chtouki M, Oukarroum A. Interactive effect of potassium and cadmium on growth, root morphology and chlorophyll a fluorescence in tomato plant. Sci Rep. 2021;11(1):5384. https://doi.org/10.1038/s41598-021-84990-4. PMID: 33686172; PMCID: PMC7940648.
16. Wu Y, Xu M, Wang P, Syeda AKR, Huang P, Dong XP. Lysosomal potassium channels. Cell Calcium. 2022;102:102536. https://doi.org/10.1016/j.ceca.2022.102536. Epub 2022 Jan 6. PMID: 35016151.
17. Fang XZ, Liu XX, Zhu YX, Ye JY, Jin CW. The $K^+$ and $NO^{3-}$ Interaction mediated by NITRATE TRANSPORTER1.1 ensures better plant growth under $K^+$-limiting conditions. Plant Physiol. 2020;184(4):1900–16. https://doi.org/10.1104/pp.20.01229. Epub 2020 Oct 22. PMID: 33093234; PMCID: PMC7723113.
18. Xu X, Du X, Wang F, Sha J, Chen Q, Tian G, Zhu Z, Ge S, Jiang Y. Effects of potassium levels on plant growth, accumulation and distribution of carbon, and nitrate metabolism in apple dwarf rootstock seedlings. Front Plant Sci. 2020;11:904. https://doi.org/10.3389/fpls.2020.00904. PMID: 32655607; PMCID: PMC7325393.
19. Vassileva M, Mendes GO, Deriu MA, Benedetto GD, Flor-Peregrin E, Mocali S, Martos V, Vassilev N, Fungi. P-solubilization, and plant nutrition. Microorganisms. 2022;10(9):1716. https://doi.org/10.3390/microorganisms10091716. PMID: 36144318; PMCID: PMC9503713.
20. Wang Y, Chen YF, Wu WH. Potassium and phosphorus transport and signaling in plants. J Integr Plant Biol. 2021;63(1):34–52. https://doi.org/10.1111/jipb.13053. PMID: 33325114.
21. Guo S, Liu Z, Sheng H, Olukayode T, Zhou Z, Liu Y, Wang M, He M, Kochian L, Qin Y. Dynamic transcriptome analysis unravels key regulatory genes of maize root growth and development in response to potassium deficiency. Planta. 2023;258(5):99. https://doi.org/10.1007/s00425-023-04260-7. PMID: 37837470; PMCID: PMC10576708.
22. Sun MG, Ma LC. Potassium-rich brine deposit in Lop nor basin, Xinjiang, China. Sci Rep. 2018;8(1):7676. https://doi.org/10.1038/s41598-018-25993-6. PMID: 29769609; PMCID: PMC5955951.
23. Deeken R, Geiger D, Fromm J, Koroleva O, Ache P, Langenfeld-Heyser R, Sauer N, May ST, Hedrich R. Loss of the *AKT2/3* potassium channel affects sugar loading into the phloem of Arabidopsis. Planta. 2002;216(2):334–44. https://doi.org/10.1007/s00425-002-0895-1. Epub 2002 Sep 21. PMID: 12447548.
24. Pilot G, Gaymard F, Mouline K, Chérel I, Sentenac H. Regulated expression of *Arabidopsis shaker* $K^+$ channel genes involved in $K^+$ uptake and distribution in the plant. Plant Mol Biol. 2003;51(5):773 – 87. https://doi.org/10.1023/a:1022597102282. PMID: 12678562.
25. Hermans C, Hammond JP, White PJ, Verbruggen N. How do plants respond to nutrient shortage by biomass allocation? Trends Plant Sci. 2006;11(12):610–7. https://doi.org/10.1016/j.tplants.2006.10.007. Epub 2006 Nov 7. PMID: 17092760.
26. Singh SP, Pandey S, Mishra N, Giri VP, Mahfooz S, Bhattacharya A, Kumari M, Chauhan P, Verma P, Nautiyal CS, Mishra A. Supplementation of Trichoderma improves the alteration of nutrient allocation and transporter genes expression in rice under nutrient deficiencies. Plant Physiol Biochem. 2019;143:351–363. doi: 10.1016/j.plaphy.2019.09.015. Epub 2019 Sep 11. PMID: 31541990.
27. Jung JY, Shin R, Schachtman DP. Ethylene mediates response and tolerance to potassium deprivation in Arabidopsis. Plant Cell. 2009;21(2):607–21. https://doi.org/10.1105/tpc.108.063099. Epub 2009 Feb 3. PMID: 19190240; PMCID: PMC2660615.

28. Wang Q, Li S, Li F, Tian X, Li Z. Identification of *Shaker* potassium channel family members in *Gossypium hirsutum* L. and characterization of *GhKAT1aD*. Life (Basel). 2023;13(7):1461. https://doi.org/10.3390/life13071461. PMID: 37511836; PMCID: PMC10381577.
29. Lu Y, Yu M, Jia Y, Yang F, Zhang Y, Xu X, Li X, Yang F, Lei J, Wang Y, Yang G. Structural basis for the activity regulation of a potassium channel AKT1 from *Arabidopsis*. Nat Commun. 2022;13(1):5682. https://doi.org/10.1038/s41467-022-33420-8. PMID: 36167696; PMCID: PMC9515098.
30. Ródenas R, García-Legaz MF, López-Gómez E, Martínez V, Rubio F, Ángeles Botella M. $NO^{3-}$, $PO_4^{3-}$ and $SO_4^{2-}$ deprivation reduced LKT1-mediated low-affinity $K^+$ uptake and SKOR-mediated $K^+$ translocation in tomato and *Arabidopsis* plants. Physiol Plant. 2017;160(4):410–424. https://doi.org/10.1111/ppl.12558. Epub 2017 May 3. PMID: 28244226.
31. Lebaudy A, Véry AA, Sentenac H. $K^+$ channel activity in plants: genes, regulations and functions. FEBS Lett. 2007;581(12):2357-66. https://doi.org/10.1016/j.febslet.2007.03.058. Epub 2007 Mar 30. PMID: 17418142.
32. Shen C, Yuan J. Genome-wide investigation and expression analysis of $K^+$-transport-related gene families in Chinese Cabbage (*Brassica rapa* ssp. pekinensis). Biochem Genet. 2021;59(1):256–82. https://doi.org/10.1007/s10528-020-10004-z. Epub 2020 Sep 29. PMID: 32990910.
33. Zhang B, Guo Y, Wang H, Wang X, Lv M, Yang P, Zhang L. Identification and characterization of *Shaker* $K^+$ channel gene family in foxtail millet (*Setaria italica*) and their role in stress response. Front Plant Sci. 2022;13:907635. https://doi.org/10.3389/fpls.2022.907635. PMID: 35755660; PMCID: PMC9218596.
34. Chen G, Chen Q, Qi K, Xie Z, Yin H, Wang P, Wang R, Huang Z, Zhang S, Wang L, Wu J. Identification of *Shaker* $K^+$ channel family members in *Rosaceae* and a functional exploration of PbrKAT1. Planta. 2019;250(6):1911–25. https://doi.org/10.1007/s00425-019-03275-3. Epub 2019 Sep 16. PMID: 31523779.
35. Jin R, Zhang A, Sun J, Chen X, Liu M, Zhao P, Jiang W, Tang Z. Identification of *Shaker* $K^+$ channel family members in sweetpotato and functional exploration of IbAKT1. Gene. 2021;768:145311. https://doi.org/10.1016/j.gene.2020.145311. Epub 2020 Nov 18. PMID: 33220344.
36. Feng C, He C, Wang Y, Xu H, Xu K, Zhao Y, Yao B, Zhang Y, Zhao Y, Idrice Carther KF, Luo J, Sun D, Gao H, Wang F, Li X, Liu W, Dong Y, Wang N, Zhou Y, Li H. Genome-wide identification of soybean *Shaker* $K^+$ channel gene family and functional characterization of GmAKT1 in transgenic *Arabidopsis thaliana* under salt and drought stress. J Plant Physiol. 2021;266:153529. https://doi.org/10.1016/j.jplph.2021.153529. Epub 2021 Sep 22. PMID: 34583134.
37. Chen C, Chen H, Zhang Y, Thomas HR, Frank MH, He Y, Xia R. TBtools: an integrative toolkit developed for interactive analyses of big biological data. Mol Plant. 2020;13(8):1194–202. https://doi.org/10.1016/j.molp.2020.06.009. Epub 2020 Jun 23. PMID: 32585190.
38. Potter SC, Luciani A, Eddy SR, Park Y, Lopez R, Finn RD. HMMER web server: 2018 update. Nucleic Acids Res. 2018;46(W1): W200-W204. https://doi.org/10.1093/nar/gky448. PMID: 29905871; PMCID: PMC6030962.
39. Xi D, Yin T, Han P, Yang X, Zhang M, Du C, Zhang H, Liu X. Genome-wide identification of sweet orange WRKY transcription factors and analysis of their expression in response to infection by *Penicillium Digitatum*. Curr Issues Mol Biol. 2023;45(2):1250–71. https://doi.org/10.3390/cimb45020082. PMID: 36826027; PMCID: PMC9954951.
40. Horton P, Park KJ, Obayashi T, Fujita N, Harada H, Adams-Collier CJ, Nakai K. WoLF PSORT: protein localization predictor. Nucleic Acids Res. 2007;35(Web Server issue): W585-7. https://doi.org/10.1093/nar/gkm259. Epub 2007 May 21. PMID: 17517783; PMCID: PMC1933216.
41. Xu B, Chen B, Qi X, Liu S, Zhao Y, Tang C, Meng X. Genome-wide identification and expression analysis of *RcMYB* genes in *Rhodiola crenulata*. Front Genet. 2022;13:831611. https://doi.org/10.3389/fgene.2022.831611. PMID: 35432456; PMCID: PMC9008588.
42. Tian C, Wan P, Sun S, Li J, Chen M. Genome-wide analysis of the GRAS gene family in rice and Arabidopsis. Plant Mol Biol. 2004;54(4):519 – 32. https://doi.org/10.1023/B:PLAN.0000038256.89809.57. PMID: 15316287.
43. Katoh K, Standley DM. MAFFT multiple sequence alignment software version 7: improvements in performance and usability. Mol Biol Evol. 2013;30(4):772–80. https://doi.org/10.1093/molbev/mst010. Epub 2013 Jan 16. PMID: 23329690; PMCID: PMC3603318.
44. Kearse M, Moir R, Wilson A, Stones-Havas S, Cheung M, Sturrock S, Buxton S, Cooper A, Markowitz S, Duran C, Thierer T, Ashton B, Meintjes P, Drummond A. Geneious Basic: an integrated and extendable desktop software platform for the organization and analysis of sequence data. Bioinformatics. 2012;28(12):1647–9. https://doi.org/10.1093/bioinformatics/bts199. Epub 2012 Apr 27. PMID: 22543367; PMCID: PMC3371832.
45. Marchler-Bauer A, Anderson JB, Chitsaz F, Derbyshire MK, DeWeese-Scott C, Fong JH, Geer LY, Geer RC, Gonzales NR, Gwadz M, He S, Hurwitz DI, Jackson JD, Ke Z, Lanczycki CJ, Liebert CA, Liu C, Lu F, Lu S, Marchler GH, Mullokandov M, Song JS, Tasneem A, Thanki N, Yamashita RA, Zhang D, Zhang N, Bryant SH. CDD: specific functional annotation with the conserved domain database. Nucleic Acids Res. 2009;37(Database issue):D205–10. https://doi.org/10.1093/nar/gkn845. Epub 2008 Nov 4. PMID: 18984618; PMCID: PMC2686570.
46. Bailey TL, Williams N, Misleh C, Li WW. MEME: discovering and analyzing DNA and protein sequence motifs. Nucleic Acids Res. 2006;34(Web Server issue): W369-73. https://doi.org/10.1093/nar/gkl198. PMID: 16845028; PMCID: PMC1538909.
47. Lescot M, Déhais P, Thijs G, Marchal K, Moreau Y, Van de Peer Y, Rouzé P, Rombauts S. PlantCARE, a database of plant cis-acting regulatory elements and a portal to tools for in silico analysis of promoter sequences. Nucleic Acids Res. 2002;30(1):325–7. https://doi.org/10.1093/nar/30.1.325. PMID: 11752327; PMCID: PMC99092.
48. Cantalapiedra CP, Hernández-Plaza A, Letunic I, Bork P, Huerta-Cepas J. eggNOG-mapper v2: functional annotation, orthology assignments, and domain prediction at the metagenomic scale. Mol Biol Evol. 2021;38(12):5825–9. https://doi.org/10.1093/molbev/msab293. PMID: 34597405; PMCID: PMC8662613.
49. Yin T, Han P, Xi D, Yu W, Zhu L, Du C, Yang N, Liu X, Zhang H. Genome-wide identification, characterization, and expression profile ofNBS-LRRgene family in sweet orange (citrussinensis). Gene. 2023;854:147117. https://doi.org/10.1016/j.gene.2022.147117. Epub 2022 Dec 13. PMID: 36526123.
50. Wu M, Jiang M, Hunag K, Tang J, Liu P. Effects of mineral elements on the proliferation of Hongyang kiwifruit group-cultured seedlings[J]. Resource Dev Market 2020,36(11):1263–6.
51. Cao X, Hu L, Chen X, Zhang R, Cheng D, Li H, Xu Z, Li L, Zhou Y, Liu A, Song J, Liu C, Liu J, Zhao Z, Chen M, Ma Y. Genome-wide analysis and identification of the low potassium stress responsive gene SiMYB3 in foxtail millet (Setariaitalica L). BMC Genomics. 2019;20(1):136. https://doi.org/10.1186/s12864-019-5519-2. PMID: 30767761; PMCID: PMC6377754.
52. Haas BJ, Papanicolaou A, Yassour M, Grabherr M, Blood PD, Bowden J, Couger MB, Eccles D, Li B, Lieber M, MacManes MD, Ott M, Orvis J, Pochet N, Strozzi F, Weeks N, Westerman R, William T, Dewey CN, Henschel R, LeDuc RD, Friedman N, Regev A. De novo transcript sequence reconstruction from RNA-seq using the Trinity platform for reference generation and analysis. Nat Protoc. 2013;8(8):1494–512. https://doi.org/10.1038/nprot.2013.084. Epub 2013 Jul 11. PMID: 23845962; PMCID: PMC3875132.
53. Liou L, Hornburg M, Robertson DS. Global FDR control across multiple RNA-seq experiments. Bioinformatics. 2023;39(1):btac718. https://doi.org/10.1093/bioinformatics/btac718. PMID: 36326442; PMCID: PMC9805573.
54. Walker DJ, Leigh RA, Miller AJ. Potassium homeostasis in vacuolate plant cells. Proc Natl Acad Sci U S A. 1996;93(19):10510–4. https://doi.org/10.1073/pnas.93.19.10510. PMID: 11607707; PMCID: PMC38416.
55. Siddoway B, Hou H, Yang J, Sun L, Yang H, Wang GY, Xia H. Potassium channel Kv2.1 is regulated through protein phosphatase-1 in response to increases in synaptic activity. Neurosci Lett. 2014;583:142–7. https://doi.org/10.1016/j.neulet.2014.08.051. Epub 2014 Sep 8. PMID: 25220706; PMCID: PMC8221410.
56. Papazian DM, Schwarz TL, Tempel BL, Jan YN, Jan LY. Cloning of genomic and complementary DNA from *Shaker*, a putative potassium channel gene from Drosophila. Science. 1987;237(4816):749 – 53. https://doi.org/10.1126/science.2441470. PMID: 2441470.
57. Reintanz B, Szyroki A, Ivashikina N, Ache P, Godde M, Becker D, Palme K, Hedrich R. AtKC1, a silent *Arabidopsis* potassium channel alpha -subunit modulates root hair $K^+$ influx. Proc Natl Acad Sci U S A. 2002;99(6):4079–84. https://doi.org/10.1073/pnas.052677799. PMID: 11904452; PMCID: PMC122651.
58. Shi T, Huang H, Barker MS. Ancient genome duplications during the evolution of kiwifruit (*Actinidia*) and related Ericales. Ann Bot. 2010;106(3):497–504. https://doi.org/10.1093/aob/mcq129. Epub 2010 Jun 24. PMID: 20576738; PMCID: PMC2924827.
59. Yang F, Wang T, Liu L. Pollen germination is impaired by disruption of a *Shaker* $K^+$ channel OsAKT1.2 in rice. J Plant Physiol. 2020;248:153140. https://doi.org/10.1016/j.jplph.2020.153140. Epub 2020 Feb 22. PMID: 32114250.
60. Feng X, Liu W, Cao F, Wang Y, Zhang G, Chen ZH, Wu F. Overexpression of HvAKT1 improves drought tolerance in barley by regulating root ion homeostasis and ROS and NO signaling. J Exp Bot. 2020;71(20):6587–600. https://doi.org/10.1093/jxb/eraa354.
61. Hosy E, Vavasseur A, Mouline K, Dreyer I, Gaymard F, Porée F, Boucherez J, Lebaudy A, Bouchez D, Very AA, Simonneau T, Thibaud JB, Sentenac H. The *Arabidopsis* outward $K^+$ channel GORK is involved in regulation of

stomatal movements and plant transpiration. Proc Natl Acad Sci U S A. 2003;100(9):5549–54. https://doi.org/10.1073/pnas.0733970100.
62. Lebaudy A, Vavasseur A, Hosy E, Dreyer I, Leonhardt N, Thibaud JB, Véry AA, Simonneau T, Sentenac H. Plant adaptation to fluctuating environment and biomass production are strongly dependent on guard cell potassium channels. Proc Natl Acad Sci U S A. 2008;105(13):5271–6. https://doi.org/10.1073/pnas.0709732105.
63. Andersen EJ, Nepal MP, Purintun JM, Nelson D, Mermigka G, Sarris PF. Wheat disease resistance genes and their diversification through integrated domain fusions. Front Genet. 2020;11:898. https://doi.org/10.3389/fgene.2020.00898.
64. Hernandez-Garcia CM, Finer JJ. Identification and validation of promoters and cis-acting regulatory elements. Plant Sci. 2014;217–218:109 – 19. https://doi.org/10.1016/j.plantsci.2013.12.007
65. Baxter L, Jironkin A, Hickman R, Moore J, Barrington C, Krusche P, Dyer NP, Buchanan-Wollaston V, Tiskin A, Beynon J, Denby K, Ott S. Conserved noncoding sequences highlight shared components of regulatory networks in dicotyledonous plants. Plant Cell. 2012;24(10):3949–65. https://doi.org/10.1105/tpc.112.103010.
66. Ma Y, Cao J, He J, Chen Q, Li X, Yang Y. Molecular mechanism for the regulation of ABA homeostasis during plant development and stress responses. Int J Mol Sci. 2018;19(11):3643. https://doi.org/10.3390/ijms19113643. PMID: 30463231; PMCID: PMC6274696.
67. Osakabe Y, Yamaguchi-Shinozaki K, Shinozaki K, Tran LP. ABA control of plant macroelement membrane transport systems in response to water deficit and high salinity. New Phytol. 2014;202(1):35–49. https://doi.org/10.1111/nph.12613. Epub 2013 Nov 28. PMID: 24283512.
68. Berens ML, Berry HM, Mine A, Argueso CT, Tsuda K. Evolution of hormone signaling networks in plant defense. Annu Rev Phytopathol. 2017;55:401–425. https://doi.org/10.1146/annurev-phyto-080516-035544. Epub 2017 Jun 23. PMID: 28645231.
69. Laura B, Silvia P, Francesca F, Benedetta S, Carla C. Epigenetic control of defense genes following MeJA-induced priming in rice (*O. sativa*). J Plant Physiol. 2018;228:166–77. https://doi.org/10.1016/j.jplph.2018.06.007. Epub 2018 Jun 13. PMID: 29936261.
70. Cao S, Cai Y, Yang Z, Joyce DC, Zheng Y. Effect of MeJA treatment on polyamine, energy status and anthracnose rot of loquat fruit. Food Chem. 2014;145:86 – 9. doi: 10.1016/j.foodchem.2013.08.019. Epub 2013 Aug 11. PMID: 24128452.
71. Olive MR, Walker JC, Singh K, Dennis ES, Peacock WJ. Functional properties of the anaerobic responsive element of the maize Adh1 gene. Plant Mol Biol. 1990;15(4):593–604. https://doi.org/10.1007/BF00017834. PMID: 2102377.
72. Yanhui C, Xiaoyuan Y, Kun H, Meihua L, Jigang L, Zhaofeng G, Zhiqiang L, Yunfei Z, Xiaoxiao W, Xiaoming Q, Yunping S, Li Z, Xiaohui D, Jingchu L, Xing-Wang D, Zhangliang C, Hongya G, Li-Jia Q. The MYB transcription factor superfamily of Arabidopsis: expression analysis and phylogenetic comparison with the rice MYB family. Plant Mol Biol. 2006;60(1):107 – 24. https://doi.org/10.1007/s11103-005-2910-y. PMID: 16463103.
73. Dubos C, Stracke R, Grotewold E, Weisshaar B, Martin C, Lepiniec L. MYB transcription factors in Arabidopsis. Trends Plant Sci. 2010;15(10):573–81. Epub 2010 Jul 30. PMID: 20674465.
74. Lin X. Common deficiency symptoms in kiwifruit and their control measures[J]. Shanghai Agricultural Sci Technol,2001(04):64–49.
75. Zhang X, Jiang H, Wang H, Cui J, Wang J, Hu J, Guo L, Qian Q, Xue D. Transcriptome analysis of rice seedling roots in response to potassium deficiency. Sci Rep. 2017;7(1):5523. https://doi.org/10.1038/s41598-017-05887-9. PMID: 28717149; PMCID: PMC5514036.
76. Pang G, Chen G, Li N. Several common deficiencies and their control in kiwifruit orchards in Xixia County[J]. Modern Agriculture,2020(06):50–1.https://doi.org/10.14070/j.cnki.15-1098.2020.06.036
77. Basset M, Conejero G, Lepetit M, Fourcroy P, Sentenac H. Organization and expression of the gene coding for the potassium transport system AKT1 of *Arabidopsis thaliana*. Plant Mol Biol. 1995;29(5):947 – 58. https://doi.org/10.1007/BF00014968. PMID: 8555458.
78. Wang Y, He L, Li HD, Xu J, Wu WH. Potassium channel alpha-subunit AtKC1 negatively regulates AKT1-mediated K(+) uptake in *Arabidopsis* roots under low-K(+) stress. Cell Res. 2010;20(7):826–37. Epub 2010 Jun 1. PMID: 20514083.
79. Zhang X, Ma J, Berkowitz GA. Evaluation of functional interaction between K(+) channel alpha- and beta-subunits and putative inactivation gating by co-expression in *Xenopus laevis* oocytes. Plant Physiol. 1999;121(3):995–1002. https://doi.org/10.1104/pp.121.3.995. PMID: 10557249; PMCID: PMC59464.
80. Sottocornola B, Visconti S, Orsi S, Gazzarrini S, Giacometti S, Olivari C, Camoni L, Aducci P, Marra M, Abenavoli A, Thiel G, Moroni A. The potassium channel KAT1 is activated by plant and animal 14-3-3 proteins. J Biol Chem. 2006;281(47):35735–41. https://doi.org/10.1074/jbc.M603361200. Epub 2006 Sep 21. PMID: 16990282.
81. Kim EJ, Kwak JM, Uozumi N, Schroeder JI. AtKUP1: an *Arabidopsis* gene encoding high-affinity potassium transport activity. Plant Cell. 1998;10(1):51–62. https://doi.org/10.1105/tpc.10.1.51. PMID: 9477571; PMCID: PMC143935.
82. Ahn SJ, Shin R, Schachtman DP. Expression of KT/KUP genes in *Arabidopsis* and the role of root hairs in $K^+$ uptake. Plant Physiol. 2004;134(3):1135–45. https://doi.org/10.1104/pp.103.034660. Epub 2004 Feb 26. PMID: 14988478; PMCID: PMC389937.
83. Ahmad R, Anjum MA. Physiological and molecular basis of salinity tolerance in fruit crops.Fruit crops. Elsevier; 2020. pp. 445–64.
84. Drain A, Thouin J, Wang L, Boeglin M, Pauly N, Nieves-Cordones M, Gaillard I, Véry AA, Sentenac H. Functional characterization and physiological roles of the single *Shaker* outward $K^+$ channel in *Medicago truncatula*. Plant J. 2020;102(6):1249–65. https://doi.org/10.1111/tpj.14697. Epub 2020 Mar 2. PMID: 31958173.

## Publisher's note